no cytotoxicity or genotoxicity due to the AG formed in the cells was found in the present study. Therefore, because AG appeared not to be a causal factor of the toxicity in vitro, additional work addressing a possible immune-mediated toxicity will be needed to clarify the toxicity of AG. This study provides new insight into the evaluation of acyl glucuronide toxicity in drug development.

Acknowledgments

We acknowledge Dr. Tetsushi Watanabe (Kyoto Pharmaceutical University) for technical teaching and discussion about the comet assay and Brent Bell for reviewing the manuscript.

Authorship Contributions

Participated in research design: Koga, Nakajima, and Yokoi.

Conducted experiments: Koga.

Contributed new reagents or analytic tools: Koga and Fujiwara.

Performed data analysis: Koga.

Wrote or contributed to the writing of the manuscript: Koga and Yokoi.

References

Ashby J, Brady A, Elcombe CR, Elliot BM, Ishamael J, Odum J, Tugwood JD, Kettle S, and Purchase IFH (1994) Mechanistically-based human hazard assessment of peroxisome proliferator-induced hepatocarcinogenesis. *Hum Exp Toxicol* **13 (Suppl 2)**:S1–S117.

Bailey MJ and Dickinson RG (2003) Acyl glucuronide reactivity in perspective: biological consequences. *Chem Biol Interact* **145**:117–137.

Banks AT, Zimmerman HJ, Ishak KG, and Harter JG (1995) Diclofenac-associated hepatotoxicity: analysis of 180 cases reported to the Food and Drug Administration as adverse reactions. *Hepatology* **22**:820–827.

Boelsterli UA (2003) Diclofenac-induced liver injury: a paradigm of idiosyncratic drug toxicity. *Toxicol Appl Pharmacol* **192**:307–322.

Boelsterli UA, Zimmerman HJ, and Kretz-Rommel A (1995) Idiosyncratic liver toxicity of nonsteroidal antiinflammatory drugs: molecular mechanisms and pathology. *Crit Rev Toxicol* **25**:207–235.

Brambilla G and Martelli A (2009) Genotoxicity and carcinogenicity studies of analgesics, anti-inflammatory drugs and antipyretics. *Pharmacol Res* **60**:1–17.

Castillo M and Smith PC (1995) Disposition and reactivity of ibuprofen and ibufenac acyl glucuronides in vivo in the rhesus monkey and in vitro with human serum albumin. *Drug Metab Dispos* **23**:566–572.

Cuthbert MF (1974) Adverse reactions to non-steroidal antirheumatic drugs. *Curr Med Res Opin* **2**:600–610.

Foster RT, Jamali F, Russell AS, and Alballa SR (1988) Pharmacokinetics of ketoprofen enantiomers in young and elderly arthritic patients following single and multiple doses. *J Pharm Sci* **77**:191–195.

Fujiwara R, Nakajima M, Yamanaka H, Nakamura A, Katoh M, Ikushiro S, Sakaki T, and Yokoi T (2007a) Effects of coexpression of UGT1A9 on enzymatic activities of human UGT1A isoforms. *Drug Metab Dispos* **35**:747–757.

Fujiwara R, Nakajima M, Yamanaka H, Katoh M, and Yokoi T (2007b) Interactions between human UGT1A1, UGT1A4, and UGT1A6 affect their enzymatic activities. *Drug Metab Dispos* **35**:1781–1787.

Hagmann W, Nies AT, König J, Frey M, Zentgraf H, and Keppler D (1999) Purification of the human apical conjugate export pump MRP2 reconstitution and functional characterization as substrate-stimulated ATPase. *Eur J Biochem* **265**:281–289.

Hirano M, Maeda K, Shitara Y, and Sugiyama Y (2004) Contribution of OATP2 (OATP1B1) and OATP8 (OATP1B3) to the hepatic uptake of pitavastatin in humans. *J Pharmacol Exp Ther* **311**:139–146.

Kohn KW (1991) Principles and practice of DNA filter elution. *Pharmacol Ther* **49**:55–77.

Kubota T, Lewis BC, Elliot DJ, Mackenzie PI, and Miners JO (2007) Critical roles of residues 36 and 40 in the phenol and tertiary amine aglycone substrate selectivities of UDP-glucuronosyltransferases 1A3 and 1A4. *Mol Pharmacol* **72**:1054–1062.

Kumar S, Samuel K, Subramanian R, Braun MP, Stearns RA, Chiu SH, Evans DC, and Baillie TA (2002) Extrapolation of diclofenac clearance from in vitro microsomal metabolism data: role of acyl glucuronidation and sequential oxidative metabolism of the acyl glucuronide. *J Pharmacol Exp Ther* **303**:969–978.

Lagas JS, Sparidans RW, Wagenaar E, Beijnen JH, and Schinkel AH (2010) Hepatic clearance of reactive glucuronide metabolites of diclofenac in the mouse is dependent on multiple ATP-binding cassette efflux transporters. *Mol Pharmacol* **77**:687–694.

Nakajima M, Koga T, Sakai H, Yamanaka H, Fujiwara R, and Yokoi T (2010) *N*-Glycosylation plays a role in protein folding of human UGT1A9. *Biochem Pharmacol* **79**:1165–1172.

Nishiyama T, Izawa T, Usami M, Ohnuma T, Ogura K, and Hiratsuka A (2010) Cooperation of NAD(P)H:quinone oxidoreductase 1 and UDP-glucuronosyltransferases reduces menadione cytotoxicity in HEK293 cells. *Biochem Biophys Res Commun* **394**:459–463.

Pirmohamed M, Madden S, and Park BK (1996) Idiosyncratic drug reactions. Metabolic bioactivation as a pathogenic mechanism. *Clin Pharmacokinet* **31**:215–230.

Riedmaier S, Klein K, Hofmann U, Keskitalo JE, Neuvonen PJ, Schwab M, Niemi M, and Zanger UM (2010) UDP-glucuronosyltransferase (UGT) polymorphisms affect atorvastatin lactonization in vitro and in vivo. *Clin Pharmacol Ther* **87**:65–73.

Riley TR 3rd and Smith JP (1998) Ibuprofen-induced hepatotoxicity in patients with chronic hepatitis C: a case series. *Am J Gastroenterol* **93**:1563–1565.

Ritter JK (2000) Roles of glucuronidation and UDP-glucuronosyltransferases in xenobiotic bioactivation reactions. *Chem Biol Interact* **129**:171–193.

Sakaguchi K, Green M, Stock N, Reger TS, Zunic J, and King C (2004) Glucuronidation of carboxylic acid containing compounds by UDP-glucuronosyltransferase isoforms. *Arch Biochem Biophys* **424**:219–225.

Sallustio BC, Degraaf YC, Weekley JS, and Burcham PC (2006) Bioactivation of carboxylic acid compounds by UDP-glucuronosyltransferases to DNA-damaging intermediates: role of glycoxidation and oxidative stress in genotoxicity. *Chem Res Toxicol* **19**:683–691.

Sallustio BC, Harkin LA, Mann MC, Krivickas SJ, and Burcham PC (1997) Genotoxicity of acyl glucuronide metabolites formed from clofibric acid and gemfibrozil: a novel role for phase-II-mediated bioactivation in the hepatocarcinogenicity of the parent aglycones? *Toxicol Appl Pharmacol* **147**:459–464.

Seitz S and Boelsterli UA (1998) Diclofenac acyl glucuronide, a major biliary metabolite, is directly involved in small intestinal injury in rats. *Gastroenterology* **115**:1476–1482.

Shipkova M, Armstrong VW, Oellerich M, and Wieland E (2003) Acyl glucuronide drug metabolites: toxicological and analytical implications. *Ther Drug Monit* **25**:1–16.

Singh NP, McCoy MT, Tice RR, and Schneider EL (1988) A simple technique for quantitation of low levels of DNA damage in individual cells. *Exp Cell Res* **175**:184–191.

Southwood HT, DeGraaf YC, Mackenzie PI, Miners JO, Burcham PC, and Sallustio BC (2007) Carboxylic acid drug-induced DNA nicking in HEK293 cells expressing human UDP-glucuronosyltransferases: role of acyl glucuronide metabolites and glycation pathways. *Chem Res Toxicol* **20**:1520–1527.

Tang W, Stearns RA, Wang RW, Chiu SH, and Baillie TA (1999) Roles of human hepatic cytochrome P450s 2C9 and 3A4 in the metabolic activation of diclofenac. *Chem Res Toxicol* **12**:192–199.

Vree TB, Van Den Biggelaar-Martea M, Verwey-Van Wissen CP, Vree ML, and Guelen PJ (1993) The pharmacokinetics of naproxen, its metabolite *O*-desmethylnaproxen, and their acyl glucuronides in humans. Effect of cimetidine. *Br J Clin Pharmacol* **35**:467–472.

Wade LT, Kenna JG, and Caldwell J (1997) Immunochemical identification of mouse hepatic protein adducts derived from the nonsteroidal anti-inflammatory drugs diclofenac, sulindac, and ibuprofen. *Chem Res Toxicol* **10**:546–555.

Walker AM (1997) Quantitative studies of the risk of serious hepatic injury in persons using nonsteroidal antiinflammatory drugs. *Arthritis Rheum* **40**:201–208.

Zeng H, Liu G, Rea PA, and Kruh GD (2000) Transport of amphipathic anions by human multidrug resistance protein 3. *Cancer Res* **60**:4779–4784.

Address correspondence to: Dr. Yokoi Tsuyoshi, Drug Metabolism and Toxicology, Faculty of Pharmaceutical Sciences, Kanazawa University, Kakuma-machi, Kanazawa 920-1192, Japan. E-mail: tyokoi@kenroku.kanazawa-u.ac.jp

Toxicology Letters 200 (2011) 139–145

Contents lists available at ScienceDirect

Toxicology Letters

journal homepage: www.elsevier.com/locate/toxlet

IL-4 mediates dicloxacillin-induced liver injury in mice

Satonori Higuchi[a], Masanori Kobayashi[a], Yukitaka Yoshikawa[a], Koichi Tsuneyama[b], Tatsuki Fukami[a], Miki Nakajima[a], Tsuyoshi Yokoi[a,*]

[a] Drug Metabolism and Toxicology, Faculty of Pharmaceutical Sciences, Kanazawa University, Kakuma-machi, Kanazawa 920-1192, Japan
[b] Department of Diagnostic Pathology, Graduate School of Medicine and Pharmaceutical Science for Research, University of Toyama, Sugitani, 930-0194 Toyama, Japan

ARTICLE INFO

Article history:
Received 18 September 2010
Received in revised form
10 November 2010
Accepted 11 November 2010
Available online 19 November 2010

Keywords:
13,14-Dihydro-15-keto-prostaglandin D_2
Drug-induced liver injury
IL-4

ABSTRACT

Drug-induced liver injury (DILI) is a major problem in drug development and clinical drug therapy. In most cases, the mechanisms are still unknown. It is difficult to predict DILI in humans due to the lack of experimental animal models. Dicloxacillin, penicillinase-sensitive penicillin, rarely causes cholestatic or mixed liver injury, and there is some evidence for immunoallergic idiosyncratic reaction in human. In this study, we investigated the mechanisms of dicloxacillin-induced liver injury. Plasma ALT and total-bilirubin (T-Bil) levels were significantly increased in dicloxacillin-administered (600 mg/kg, i.p.) mice. Dicloxacillin administration induced Th2 (helper T cells)-mediated factors and increased the plasma interleukin (IL)-4 level. Neutralization of IL-4 suppressed the hepatotoxicity of dicloxacillin, and recombinant mouse IL-4 administration (0.5 or 2.0 μg/mouse, i.p.) exacerbated it. Chemoattractant receptor-homologous molecule expressed on Th2 cells (CRTh2) is a cognate receptor for prostaglandin (PG) D_2, and is suggested to be involved in Th2-dependent allergic inflammation. We investigated the effect of 13,14-Dihydro-15-keto-PGD_2 (DK-PGD_2; 10 μg/mouse, i.p.) administration on dicloxacillin-induced liver injury. DK-PGD_2/dicloxacillin coadministration resulted in a significant increase of alanine aminotransferases and a remarkable increase of macrophage inflammatory protein 2 expression. In conclusion, to the best of our knowledge, this is the first report to demonstrate that dicloxacillin-induced liver injury is mediated by a Th2-type immune reaction and exacerbated by DK-PGD_2.

1. Introduction

Drug-induced liver injury (DILI) is the most frequent reason for the withdrawal of an approved drug from the market and for failures in drug development in pharmaceutical companies. Because of DILI, several drugs have been removed from the pharmaceutical market, including bromfenac, ebrotidine, and troglitazone (Holt and Ju, 2006). In most cases, the mechanisms of DILI are unknown and predictive experimental animal models are lacking.

Adverse effects of antibiotics are variable and can induce phlebitis, hypersensitivity reactions, changes in microbial flora, adverse interactions with other drugs as well as liver injury (Stein, 2005). It has been reported that there are many case reports of DILI due to antibiotics administration (Bjornsson and Olsson, 2005), however there are a few reports of pathological investigations. Dicloxacillin and penicillinase-sensitive penicillin rarely cause liver injury and there is some evidence for an immunoallergic idiosyncratic reaction. Dicloxacillin induced cholestasis with a moderate inflammatory reaction, allergic symptoms and infiltration of mononuclear cells, such as neutrophils and eosinophils, were demonstrated in many cases (Olsson et al., 1992). Allergic symptoms and eosinophilia are generally induced by Th2 cytokines (Kay, 2001). From these lines of evidences, we hypothesized that Th2 factors might involve in dicloxacillin-induced liver injury.

T cell-mediated immune responses play pivotal roles in the pathogenesis of a variety of human liver disorders (Kita et al., 2001; Heneghan and McFarlane, 2002; Holt and Ju, 2006). The action of T cells in the liver is mediated through the release of a variety of cytokines, which target liver cells and immune cells by activating multiple signaling cascades, including the signal transducers and activators of transcription factor (STAT) family members (Leonard and O'Shea, 1998). STAT6 is specifically activated by interleukin (IL)-4, which plays important roles in Th2 differentiation, tissue adhesion, and inflammation (Jaruga et al., 2003; Nelms et al., 1999). Th cells are subdivided into Th1, Th2, and Th17 subsets by their unique production of cytokines and characteristic transcription factors. Th1 cells require "T-box expressed in T cells" (T-bet) and secrete interferon (IFN)-γ. In contrast, Th2 cells require GATA-binding domain-3 (GATA-3) and produce IL-4, IL-5 and IL-13. Retinoid-related orphan receptor γt (ROR-γt) is indispensable for the differentiation of Th17 cells which mainly secret IL-17 and IL-22 (Kidd, 2003; Steinman, 2007).

Th2-type cytokines such as IL-4 and IL-5 influence a wide range of events associated with allergic inflammation. IL-4 stimulates the

* Corresponding author. Tel./fax: +81 76 234 4407.
E-mail address: tyokoi@kenroku.kanazawa-u.ac.jp (T. Yokoi).

0378-4274/$ – see front matter © 2010 Elsevier Ireland Ltd. All rights reserved.
doi:10.1016/j.toxlet.2010.11.006

production of IgE and promotes the development of mast cells. IL-5 is involved in the development of eosinophils (Kay, 2001). In concanavalin (Con) A-mediated hepatitis, a widely accepted mouse model for studying T cell-mediated liver injury, IL-4 stimulates the secretion of Eotaxin-1 and enhances IL-5 production resulting in the attraction of neutrophils and eosinophils into the liver which leads to hepatitis (Jaruga et al., 2003).

Prostaglandin D_2 (PGD_2) is implicated in various allergic inflammatory diseases, such as atopic dermatitis, allergic asthma, and airway inflammation. It has been reported that PGD_2 has protective roles in acetaminophen-induced liver injury and 15-deoxy PGJ_2, which is metabolite of PGD_2, enhances allyl alcohol-induced hepatotoxicity (Reilly et al., 2001; Maddox et al., 2004). PGD_2 elicits biological responses by activating two receptors, the D-prostanoid receptor (DP) and the chemoattractant receptor homologous-molecule expressed on T-helper-type-2 cells (CRTh2), which are linked to different signaling pathways. CRTh2 expresses in eosinophils, basophils, and Th2 cells, but not in hepatocytes or endothelial cells. The decrease in cAMP levels and mobilization of intracellular Ca^{2+} mediated by CRTh2 activation leads to the chemotaxis of Th2 lymphocytes, eosinophils, and monocytes. 13,14-Dihydro-15-keto-prostaglandin D_2 (DK-PGD_2) is a selective CRTh2 agonist that does not activate DP, as reviewed by Kostenis and Ulven (2006). CRTh2 activation plays a significant role in Th2-dependent neutrophil inflammation (Takeshita et al., 2004). In this study, we found that dicloxacillin-induced liver injury is mediated by IL-4 and exacerbated by DK-PGD_2 in mice.

2. Materials and methods

2.1. Chemicals

Dicloxacillin was purchased from Sigma (St. Louis, MO). RNAiso was from Nippon Gene (Tokyo, Japan). Fuji DRI-CHEM slides of GPT/ALT-PIII and TBIL-PIII to measure alanine aminotransferase (ALT) and total-bilirubin (T-Bil), respectively, were from Fujifilm (Tokyo, Japan). ReverTra Ace was from Toyobo (Tokyo, Japan). Random hexamer and SYBR Premix Ex Taq were from Takara (Osaka, Japan). All primers were commercially synthesized at Hokkaido System Sciences (Sapporo, Japan). 13,14-Dihydro-15-keto-prostaglandin D_2 (DK-PGD_2) was purchased from Cayman Chemical (Denver, CO). Recombinant mouse IL-4 (rIL-4) was from Endogen (Cambridge, MA). Rabbit polyclonal antibody against myeloperoxidase (MPO) was from DAKO (Carpinteria, CA). Monoclonal anti-mouse IL-4 antibody was from U-Cytech Bioscienses (Utrecht, Netherlands). Monoclonal rat IgG2a isotype, used as a control, from R&D Systems (Abingdon, UK). A Ready-SET-GO! Mouse Interleukin-4 (IL-4) enzyme-linked immunosorbent assay (ELISA) kit was from eBioscience (San Diego, CA). Other chemicals were of analytical or the highest grade commercially available.

2.2. Mouse models of dicloxacillin-induced liver injury

Female BALB/cCrSlc mice (6 weeks old) were obtained from SLC Japan (Hamamatsu, Japan). Mice were housed in a controlled environment (temperature 25 ± 1 °C, humidity 50 ± 10%, and 12 h light/12 h dark cycle) in the institutional animal facility with access to food and water *ad libitum*. Animals were acclimatized before use for the experiments. Mice were administered intraperitoneally (i.p.) dicloxacillin (600 mg/kg, dissolved in saline) in a non-fasting condition. Six hours after dicloxacillin administration, the animals were sacrificed and the blood was collected from inferior vena cava, and liver from the biggest lobe. For measurement of the plasma IL-4 level, mice were sacrificed at 6 h after the dicloxacillin administration. A portion of each excised liver was fixed in 10% formalin neutral buffer solution and used for immunohistochemical staining. The degree of liver injury was assessed by hematoxylin–eosin (H&E) staining. Infiltration of mononuclear cells was assessed by immunostaining for MPO. Rabbit polyclonal antibody against MPO was used for immunohistochemical staining of liver as previously described (Kumada et al., 2004). Animal maintenance and treatment were conducted in accordance with the National Institutes of Health Guide for Animal Welfare of Japan, as approved by the Institutional Animal Care and Use Committee of Kanazawa University, Japan.

2.3. Real-time reverse transcription (RT)-PCR

RNA from the mouse liver was isolated using RNAiso according to the manufacturer's instructions. T-bet, GATA-3, ROR-γt, IFN-γ, IL-5, STAT1, STAT3, STAT6, Eotaxin-1, monocyte chemoattractant protein-1 (MCP-1) and macrophage inflammatory protein-2 (MIP-2) were quantified by real-time RT-PCR. The primer sequences used in this study are shown in Table 1. For the RT-process, total RNA (10 μg) and 150 ng random hexamer were mixed and incubated at 70 °C for 10 min. RNA solution was added to a reaction mixture containing 100 units of ReverTra Ace, reaction buffer and 0.5 mM dNTPs in a final volume of 40 μl. The reaction mixture was incubated at 30 °C for 10 min, 42 °C for 1 h, and heated at 98 °C for 10 min to inactivate the enzyme. The real-time RT-PCR was performed using the Mx3000P instrument (Stratagene, La Jolla, CA). The PCR mixture contained 1 μl or 2 μl of template cDNA, SYBR Premix Ex Taq solution and 8 pmol of forward and reverse primers. Amplified products were monitored directly by measuring the increase of the dye intensity of the SYBR Green I (Molecular Probes, Eugene, OR).

Table 1
Sequences of primers used for real-time RT-PCR analyses.

Gene		Sequences
mIL-5	FP	5′-AAA GAG ACC TTG ACA CAG CTG-3′
	RP	5′-CCA CGG ACA GTT TGA TTC TTC-3′
mIFN-γ	FP	5′-GGC CAT CAG CAA CAT AAG C-3′
	RP	5′-TGG ACC ACT CGG ATG AGC TCA-3′
mGATA-3	FP	5′-GGA GGA CTT CCC CAA GAG CA-3′
	RP	5′-CAT GCT GGA AGG GTG GTG A-3′
mT-bet	FP	5′-CAA GTG GGT GCA GTG TGG AAA G-3′
	RP	5′-TGG AGA GAC TGC AGG ACG ATC-3′
mROR-γt	FP	5′-ACC TCC ACT GCC AGC TGT GTG CTG TC-3′
	RP	5′-TCA TTT CTG CAC TTC TGC ATG TAG ACT GTC CC-3′
mSTAT-6	FP	5′-ATC TTC AAC GAC AAC AGC CTC A-3′
	RP	5′-GGA GAA GGC TAG TGA CAT ATT G-3′
mSTAT-1	FP	5′-GTT TCA GCT CTG CTC CAT AC-3′
	RP	5′-CTG CTG AAG CTC GAA CCA C-3′
mSTAT-3	FP	5′-TGC AGA GCA GGT ATC TTG AG-3′
	RP	5′-TGC TGC TTC TCT GTC ACT AC-3′
mEotaxin-1	FP	5′-TCC ACA GCG CTT CTA TTC CT-3′
	RP	5′-CTA TGG CTT TCA GGG TGC AT-3′
mMCP-1	FP	5′-TGT CAT GCT TCT GGG CCT G-3′
	RP	5′-CCT CTC TCT TGA GCT TGG TG-3′
mMIP-2	FP	5′-AAG TTT GCC TTG ACC CTG AAG-3′
	RP	5′-ATC AGG TAC GAT CCA GGC TTC-3′
mGAPDH	FP	5′-AAA TGG GGT GAG GCC GGT-3′
	RP	5′-ATT GCT GAC AAT CTT GAG TGA-3′

FP: forward primer, RP: reverse primer.

2.4. Administration of recombinant mouse IL-4 (rIL-4) or anti-mouse IL-4 antibody

One hour after dicloxacillin administration, rIL-4 was intraperitoneally administered (0.5 or 2.0 μg of rIL-4 in 0.2 ml of sterile PBS containing 0.5% BSA) in a non-fasting condition. As a control, vehicle was administered. In the neutralization study, mice were administered anti-mouse IL-4 antibody intraperitoneally (100 μg of anti-mouse IL-4 antibody in 0.2 ml of sterile PBS), 1 h before dicloxacillin administration. As a control, rat IgG2a was administered (100 μg of rat IgG2a in 0.2 ml of sterile PBS).

2.5. Treatment of DK-PGD_2

One hour after dicloxacillin administration, mice were administered with DK-PGD_2 intraperitoneally (10 μg/mouse, dissolved in 200 μl of PBS) in a non-fasting condition. As a control, vehicle was administered.

2.6. Measurement of plasma IL-4 level

Plasma IL-4 level was measured by enzyme-linked immunosorbent assay (ELISA) using a Ready-SET-GO! Mouse IL-4 kit according to the manufacturer's instructions.

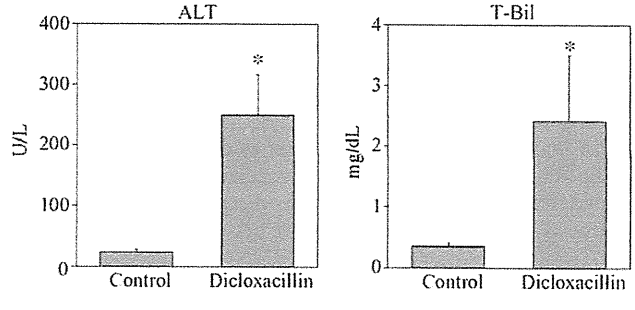

Fig. 1. Plasma ALT and T-Bil levels in dicloxacillin-administered mice. Mice were administered dicloxacillin (600 mg/kg, i.p.), and plasma for ALT and T-Bil were collected 6 h after the administration. Data are mean ± SD ($n = 4$; control, 5; dicloxacillin). Significantly different from saline-administered control mice ($^*p < 0.05$).

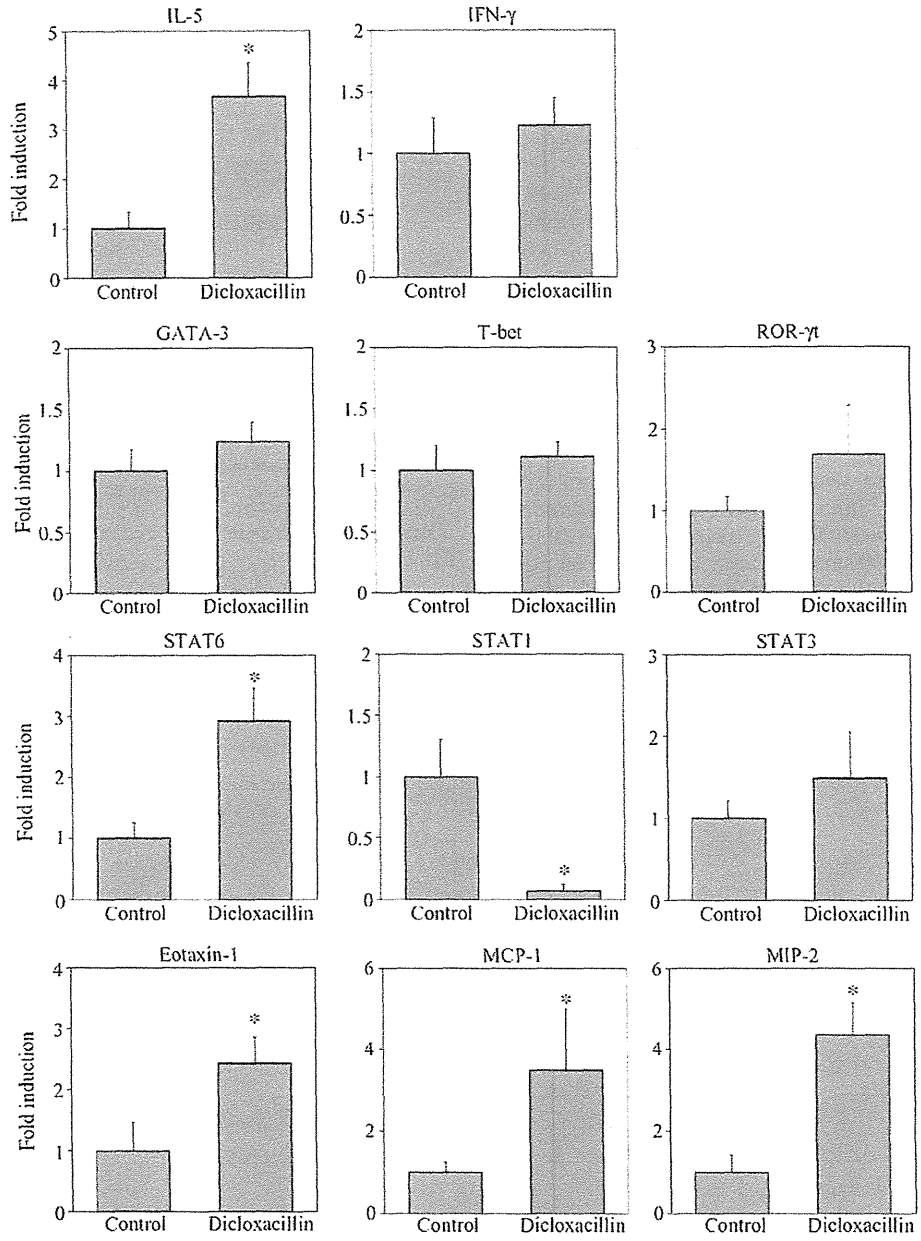

Fig. 2. Hepatic mRNA levels of transcription factors, cytokines and chemokines in dicloxacillin-administered mice. Mice were administered dicloxacillin (600 mg/kg, i.p.), and the hepatic IL-5, IFN-γ, GATA-3, T-bet, ROR-γt, STAT6, STAT1, STAT3, Eotaxin-1, MCP-1, and MIP-2 mRNA levels were measured by real-time RT-PCR 6 h after the administration. Data are mean ± SD ($n = 4$; control, 5; dicloxacillin). Significantly different from saline-administered control mice ($^*p < 0.05$).

2.7. Statistical analysis

Data are presented as mean ± SD. Statistical analyses between multiple groups were performed using one-way analysis of variance (ANOVA), followed by Tukey's post hoc test, and comparisons between two groups were carried out using two-tailed Student's *t* test in mRNA and plasma IL-4 level. In ALT and T-Bil levels, non-parametric statistical analysis was conducted using the Mann–Whitney *U* test and Kruskal–Wallis test. $p < 0.05$ was considered statistically significant.

3. Results

3.1. Increase of plasma ALT and T-Bil levels in dicloxacillin-administrated mice

Female BALB/c mice were administered dicloxacillin at a dose of 600 mg/kg. Plasma ALT and T-Bil (Fig. 1) were significantly increased 6 h after dicloxacillin administration. The administration of dicloxacillin at a dose of 400 mg/kg did not affect on the ALT and T-Bil levels (data not shown).

3.2. Expression of transcription factor, cytokine, and chemokine genes in dicloxacillin-administered mouse liver

To investigate the involvement of immunological factors in the dicloxacillin hepatotoxicity, hepatic mRNA levels of IL-5, IFN-γ, GATA-3, T-bet, ROR-γt, STAT6, STAT1, STAT3, Eotaxin-1, MCP-1, and MIP-2 were measured by real-time RT-PCR. IL-5, STAT6, Eotaxin-1, MCP-1, and MIP-2 expressions were significantly increased in dicloxacillin-administered mice compared with the control mice, whereas STAT1 expression was significantly decreased. Furthermore, T-bet, GATA-3, ROR-γt, IFN-γ, and STAT3 expressions were

not changed (Fig. 2). These results suggested that Th2-related factors, such as IL-5, STAT6, and Eotaxin-1, were involved in the dicloxacillin-induced liver injury.

3.3. Plasma IL-4 level in dicloxacillin-administered mouse liver

IL-4 is a cytokine which activates STAT6 (Nelms et al., 1999), and is a major factor in Con A-induced hepatitis (Jaruga et al., 2003). To investigate whether IL-4 was involved in the dicloxacillin-induced liver injury, we measured plasma IL-4 in dicloxacillin-administered mice (Fig. 3). Plasma IL-4 level was significantly increased in dicloxacillin-administered group compared with the control mice.

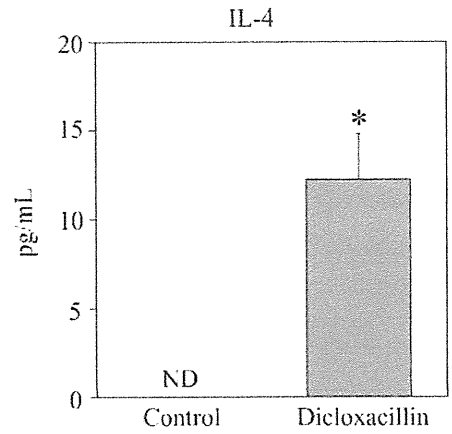

Fig. 3. Plasma IL-4 level in dicloxacillin-administered mice. Mice were administered dicloxacillin (600 mg/kg, i.p.), and plasma was collected 6 h after the administration. Data are mean ± SD ($n = 4$; control, 5; dicloxacillin). Significantly different from saline-administered control mice ($^{*}p < 0.05$).

3.4. Exacerbation of hepatotoxic effect by rIL-4 administration, and amelioration by anti-IL-4 antibody administration

To further investigate whether IL-4 was involved in the dicloxacillin-induced liver injury, we performed rIL-4 administration and IL-4 neutralization studies (Fig. 4). In the dicloxacillin/rIL-4 cotreatment study, the plasma ALT level was increased significantly and dose-dependently in mice coadministered 2.0 μg/mouse

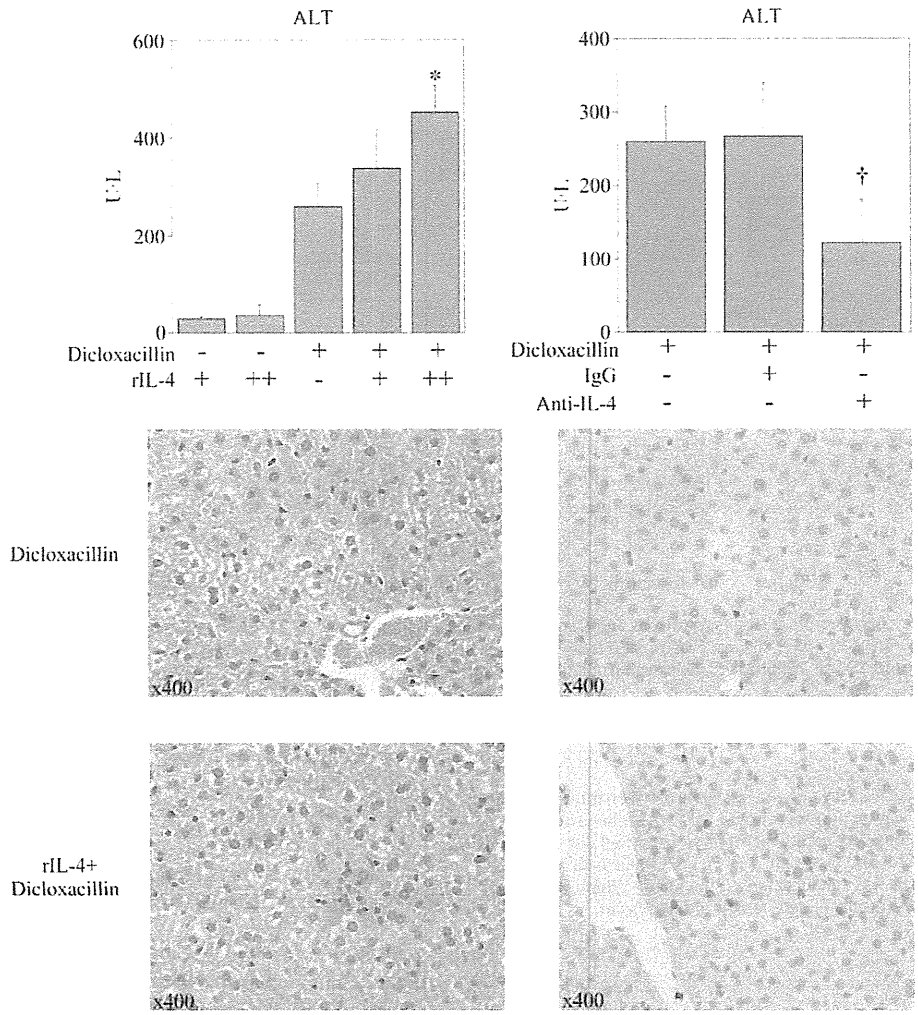

Fig. 4. Effects of recombinant mouse IL-4 (rIL-4) or anti-mouse IL-4 antibody administration on plasma ALT in dicloxacillin-administered mice. Mice were administered dicloxacillin (600 mg/kg, i.p.) and the plasma ALT was measured 6 h after the administration. In the rIL-4 administration study, rIL-4 (0.5 or 2.0 μg/mouse indicated + or ++, respectively) was administered, 1 h after dicloxacillin administration. In the IL-4 neutralization study, anti-mouse IL-4 antibody (0.1 mg/mouse, i.p.) was administered, 1 h before dicloxacillin administration. Liver specimens were prepared 6 h after the dicloxacillin administration. Liver tissue sections were stained with H&E (left photos) or immunostained with anti-MPO antibody (right photos). Data are mean ± SD ($n = 4$–5). Significantly different from dicloxacillin-administered group ($^{*}p < 0.05$); significantly different from dicloxacillin-plus control IgG2a administered group ($^{\dagger}p < 0.05$).

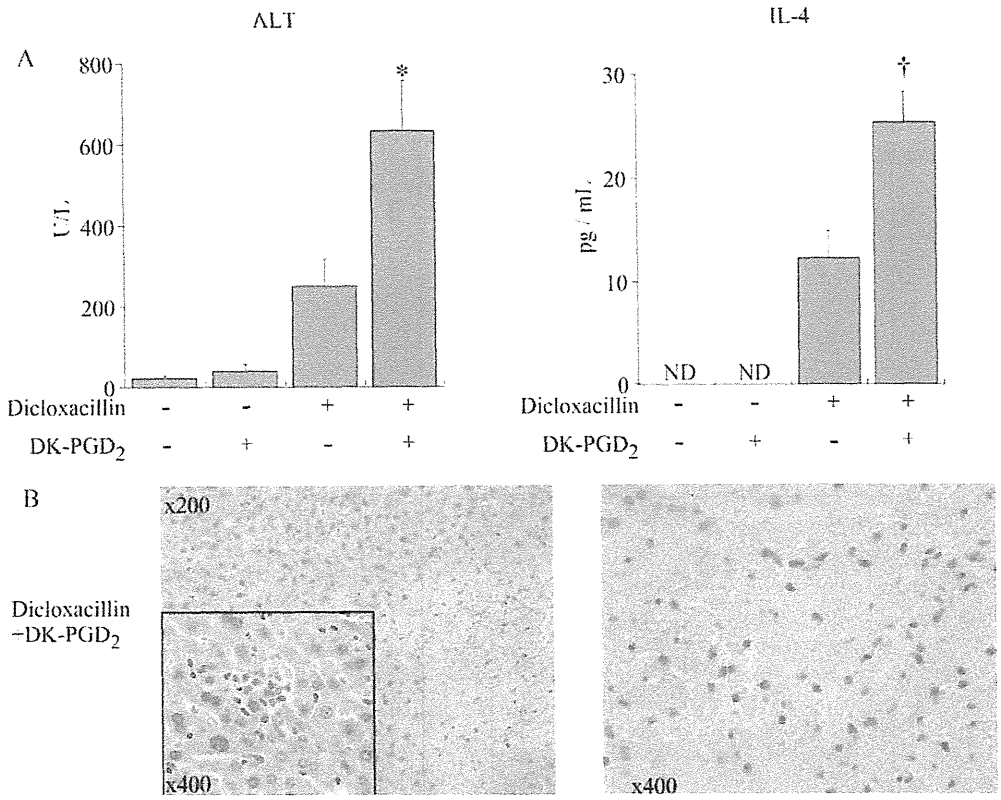

Fig. 5. Effects of DK-PGD_2 treatment on dicloxacillin-induced liver injury in mice. Mice were administered dicloxacillin (600 mg/kg, i.p.), and the plasma ALT and IL-4 levels were measured 6 h after the administration (A). One hour after dicloxacillin administration, DK-PGD_2 (10 μg/mouse, i.p.) was administered. Liver specimens (B) were prepared 6 h after the dicloxacillin administration. Liver tissue sections were stained with H&E (left photo) or immunostained with anti-MPO antibody (right photo). Data are mean ± SD (dicloxacillin and/or DK-PGD_2 administered). Significantly different from saline-administered group ($^*p < 0.05$); significantly different from dicloxacillin-administered mice ($^\dagger p < 0.05$).

rIL-4 compared with only dicloxacillin-administered mice. However, rIL-4 alone did not induce liver injury in mice. In the H&E staining, infiltration of mononuclear cells into the hepatocytes was observed in the dicloxacillin/rIL-4-coadministered group but not in the dicloxacillin-administered group. In anti-MPO staining, the numbers of MPO-positive mononuclear cells were increased in the dicloxacillin/rIL-4-coadministered group compared with dicloxacillin-administered group. In the neutralization study, the i.p. administration of anti-mouse IL-4 antibody significantly reduced the plasma ALT, but rat IgG2 treatment demonstrated no effect on the dicloxacillin-induced liver injury.

3.5. Effects of DK-PGD_2 treatment

We investigated the effects of DK-PGD_2, a selective CRTh2 agonist, on dicloxacillin-induced liver injury. Administration of DK-PGD_2 alone did not increase the plasma ALT and IL-4 levels, and DK-PGD_2 alone at a higher dose (50 μg/mouse, i.p.) did not increase ALT level (data not shown). The plasma ALT and IL-4 levels were significantly increased in the dicloxacillin/DK-PGD_2-coadministered group compared with the saline-administered group (Fig. 5A). In the histopathological study, spotty necrosis and infiltration of MPO-positive mononuclear cells were observed in the dicloxacillin/DK-PGD_2-coadministered group, but not in the dicloxacillin-administered group (Fig. 5B).

3.6. Effects on liver mRNA expressions in DK-PGD_2 administered mice

To evaluate the underlying mechanisms responsible for the increased susceptibility of DK-PGD_2 administered mice to dicloxacillin-induced liver injury, the mRNA expression levels were assessed. The hepatic mRNA levels of GATA-3, Eotaxin-1, MCP-1 and MIP-2 were significantly increased compared with the dicloxacillin-administered mice (Fig. 6). Especially, MIP-2 mRNA was markedly increased. In contrast, IFN-γ, IL-5, ROR-γt, STAT3, and STAT6 were not changed, and T-bet and STAT1 were significantly decreased (data not shown).

4. Discussion

Adverse drug reactions to antibiotics are variable, but severe liver injury is rarely reported (Bjornsson and Olsson, 2005) and the mechanism of antibiotic-induced liver injury remains to be clarified. Dicloxacillin, penicillinase-sensitive penicillin, rarely causes liver injury and there is some evidence for an immunoallergic idiosyncratic reaction (Olsson et al., 1992). In the present study, dicloxacillin-induced liver injury was investigated in mice. Firstly, we investigated the effects of dicloxacillin administration on ALT and T-Bil in normal female BALB/c mice (Fig. 1). BALB/c mice were previously used as a model for halothane-induce liver injury, which is mediated by immunological factors (Kobayashi et al., 2009). The ALT increase induced by dicloxacillin was attenuated after 24 h, compared with those after 6 h (data not shown). This is the first mice model to study dicloxacillin-induced liver injury. Flucloxacillin, which is structural homologue of dicloxacillin, has a higher incidence of liver injury than dicloxacillin (Bjornsson and Olsson, 2005; Olsson et al., 1992) and it has been recently reported that HLA allele is a major biomarker of DILI due to flucloxacillin (Daly et al., 2009), suggested that immune responses are mainly involved in flucloxacillin-induced liver injury. However, the mechanisms are unclear and there is no mouse model, we would like

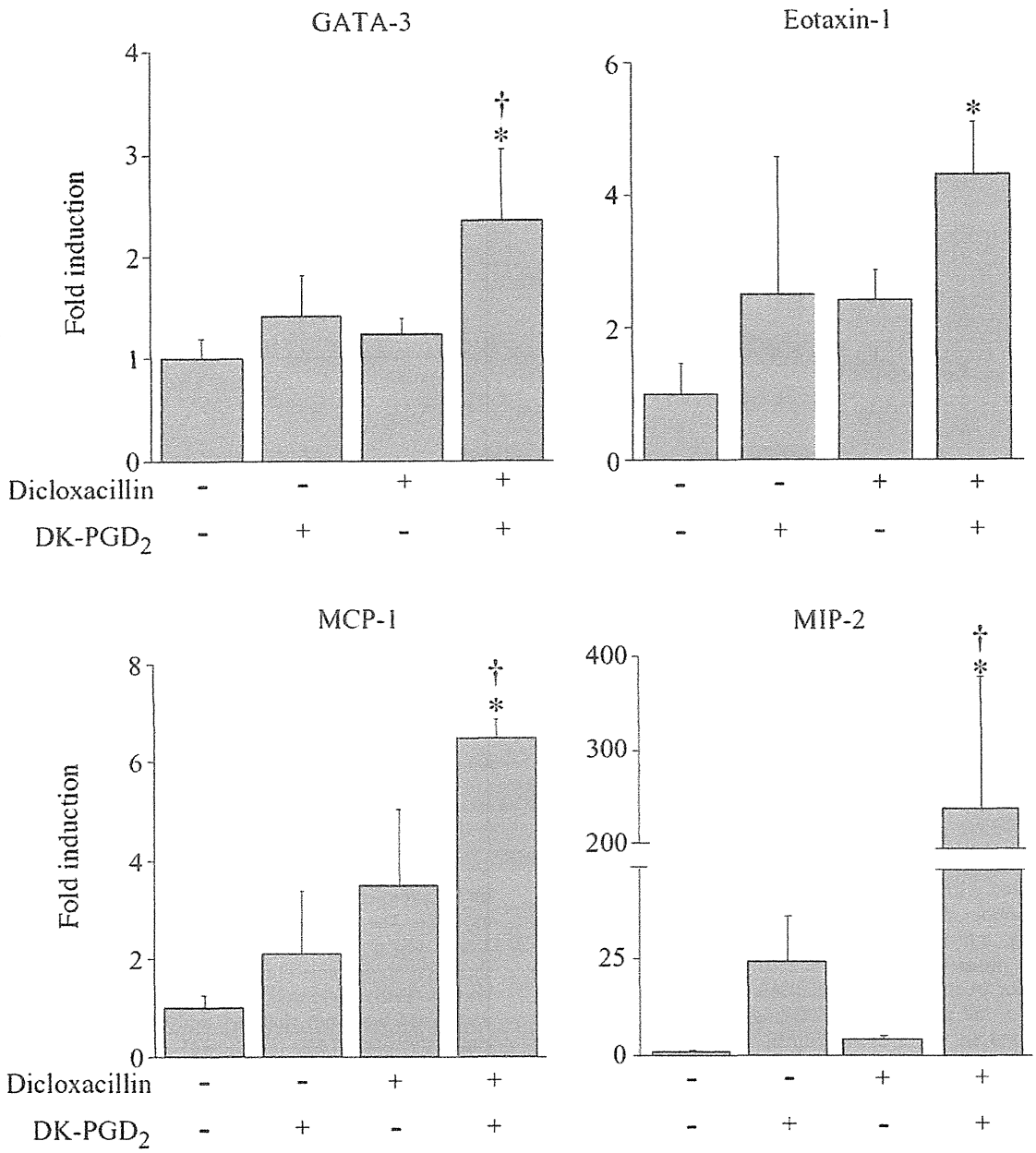

Fig. 6. Effects of DK-PGD_2 treatment on hepatic mRNA levels of transcription factor and chemokines in dicloxacillin-administered mice. Mice were administered dicloxacillin (600 mg/kg, i.p.). One hour after dicloxacillin administration, DK-PGD_2 (10 μg/mouse, i.p.) was administered. GATA-3, Eotaxin-1, MCP-1 and MIP-2 liver mRNA levels were measured by real time RT-PCR 6 h after the administration. Data are mean ± SD ($n = 4$; non-treatment, 5; dicloxacillin and/or DK-PGD_2 administered). Significantly different from saline-administered control mice (*$p < 0.05$); significantly different from dicloxacillin-administered mice (†$p < 0.05$).

to investigate whether the mechanisms of liver injury due to flucloxacillin is similar to those of dicloxacillin.

In this study, a relationship between dicloxacillin-induced liver injury and immunological factors was demonstrated (Figs. 2 and 3). The administration of dicloxacillin significantly increased the expression of hepatic IL-5, STAT6, and Eotaxin-1 mRNA, whereas it decreased STAT1 mRNA. Plasma IL-4 was induced in dicloxacillin-administered mice. These results suggest that Th2-mediated factors could be involved in dicloxacillin-induced liver injury. It has been reported that IL-4 activates STAT6 which induces IL-5 and Eotaxins-1 (Jaruga et al., 2003), and induces SOCS1 and SOCS3 which inhibit the STAT1 activity (Palmer and Restifo, 2009). The mRNA expressions of chemokines such as MCP-1 and MIP-2 were significantly increased in dicloxacillin-administered mice. MCP-1 is increased in acetaminophen-induced liver injury (Dambach et al., 2006), and MIP-2 induces neutrophil recruitment and is markedly increased in halothane-induced liver injury (Biedermann et al., 2000; Kobayashi et al., 2009). Eotaxin-1 and IL-5 are involved in allergic inflammation (Kay, 2001). These chemokines might be involved in the dicloxacillin-induced liver injury.

We demonstrated that rIL-4 exacerbated the dicloxacillin-induced liver injury, and neutralization of IL-4 significantly inhibited the increase of the plasma ALT level (Fig. 4). In liver injury, IL-4, a multifunctional Th2 cytokine, plays a protective role in ischemia/reperfusion-induced liver injury. In addition, IL-4 plays a pivotal role in Con A-induced liver injury (Kato et al., 2000; Jaruga et al., 2003), and promotes hapten-induced pro-inflammatory responses in trifluoroacetyl chloride-induced liver injury (Njoku et al., 2009). Elevated IL-4 has been reported in human liver diseases such as chronic hepatitis C (Spanakis et al., 2002) and

primary biliary cirrhosis (Harada et al., 1997). In this study, IL-4 was demonstrated to be involved in the dicloxacillin-induced liver injury.

CRTh2, one of the PGD_2 receptors, plays a major role in atopic dermatitis, allergic asthma, and airway inflammation, and it was demonstrated that CRTh2 is responsible for PGD_2 chemotaxis of Th2 cells, eosinophils, basophils, and monocytes (Kostenis and Ulven, 2006). DK-PGD_2 is a CRTh2 selective agonist that enhances Th2-type inflammation (Spik et al., 2005). In this study, Th2-mediated immune responses were suggested to be involved in the dicloxacillin-induced liver injury, thus we hypothesized that DK-PGD_2 may exacerbate liver injury. The plasma ALT level was significantly increased in the dicloxacillin/DK-PGD_2-coadministered group (Fig. 5). DK-PGD_2 enhances the chemotactic responsiveness to other chemoattractants, as well as degranulation (Kostenis and Ulven, 2006). Therefore, it was conceivable that a higher ALT level would be observed in the dicloxacillin/DK-PGD_2-coadministered group than in the rIL-4/dicloxacillin-coadministered group (Figs. 4 and 5). The hepatic GATA-3 mRNA level was significantly increased in the dicloxacillin/DK-PGD_2-coadministered group suggesting an increase in Th2-mediated factors in the liver, followed by an increase in the plasma IL-4 level (Nelms et al., 1999). Hepatic mRNA levels of Eotaxin-1, MCP-1, and MIP-2 levels were significantly increased in the dicloxacillin/DK-PGD_2-coadministered group (Fig. 6). These chemokines induce the infiltration of neutrophils followed by necrosis. Especially, MIP-2 mRNA was markedly increased, since CRTh2 activation induces MIP-2 secretion (Takeshita et al., 2004). In this study, we demonstrated that DK-PGD_2 exacerbates dicloxacillin-induced liver injury due to induction of IL-4 and MIP-2, followed by the activation of Th2 cells and other immune cells.

Although the mechanisms of DILI are still unclear due to the lack of proper animal models, LPS-treated rodents become sensitive to human hepatotoxic drugs, such as sulindac, diclofenac, chlorpromazine, and trovafloxacin (Zou et al., 2009; Shaw et al., 2009). Cytokines such as TNF-α, IL-1, IL-6, and IFN-γ are upregulated after the activation of Toll-like receptor 4 by LPS (Gaestel et al., 2009; Shaw et al., 2009), however the involvement of Th2 factors in drug-induced liver injury in LPS-administered rodents was never reported. Enhanced responsiveness with DK-PGD_2 could be a novel method in drug development to detect human hepatotoxic drugs that involve Th2-specific factors.

In conclusion, we reported that Th2 immune factors, such as IL-4, IL-5, and Eotaxin-1, were involved in drug-induced liver injury in mice, and DK-PGD_2 exacerbates dicloxacillin-induced liver injury via Th2 cytokines and chemokines. The present study provides new insight into the mechanisms of drug-induced liver injury.

Funding

Health and Labor Sciences Research Grants from the Ministry of Health, Labor and Welfare of Japan (H20-BIO-G001).

Conflict of interest

None of the authors has any conflicts of interest related to this manuscript.

Acknowledgement

We thank Mr. Brent Bell for reviewing the manuscript.

References

Biedermann, B.T., Knelling, M., Mailhammer, R., Maier, K., Sander, C.A., Kollias, G., Kunkel, S.L., Hultner, L., Rocken, M., 2000. Mast cell control neutrophil recruitment during T cell-mediated delayed hypersensitivity reactions through tumor necrosis factor and macrophage inflammatory protein 2. J. Exp. Med. 192, 1441–1451.
Bjornsson, E., Olsson, R., 2005. Outcome and prognostic markers in severe drug-induced liver disease. Hepatology 42, 481–489.
Daly, A.K., Donaldson, P.T., Bhatnagar, P., et al., 2009. HLA-B*5701 genotype is a major determinant of drug-induced liver injury due to flucloxacillin. Nat. Genet. 41, 816–819.
Dambach, D.M., Durham, S.K., Laskin, J.D., Laskin, D.L., 2006. Distinct roles of NF-κB p50 in the regulation of acetaminophen-induced inflammatory mediator production and hepatotoxicity. Toxicol. Appl. Pharmacol. 211, 157–165.
Gaestel, M., Kotlyarov, A., Kracht, M., 2009. Targeting innate immunity protein kinase signaling in inflammation. Nat. Rev. Drug. Discov. 8, 480–497.
Harada, K., Water, J.V., Leung, P.S.C., Coppel, R.L., Ansari, A., Nakanuma, Y., Gershwin, M.E., 1997. *In situ* nucleic acid hybridization of cytokines in primary biliary cirrhosis: predominance of the Th1 subset. Hepatology 25, 791–796.
Heneghan, M.A., McFarlane, I.G., 2002. Current and novel immunosuppressive therapy for autoimmune hepatitis. Hepatology 35, 7–13.
Holt, M.P., Ju, C., 2006. Mechanisms of drug-induced liver injury. AAPS J. 8, 48–54.
Jaruga, B., Hong, F., Sun, R., Radaeva, S., Gao, B., 2003. Crucial role of IL-4/STAT6 in T cell-mediated hepatitis: up-regulating eotaxins and IL-5 and recruiting leukocytes. J. Immunol. 171, 3233–3244.
Kato, A., Yoshidome, H., Edwards, M.J., Lentsch, A.B., 2000. Reduced hepatic ischemia/reperfusion injury by IL-4: potential anti-inflammatory role of STAT6. Inflamm. Res. 49, 275–279.
Kay, A.B., 2001. Allergy and allergic diseases. N. Engl. J. Med. 344, 30–37.
Kidd, P., 2003. Th1/Th2 balance: the hypothesis, its limitations, and implications for health and disease. Altern. Med. Rev. 8, 223–246.
Kita, H., Macky, I.R., Van, D.W.J., Gershwin, M.E., 2001. The lymphoid liver: considerations on pathways to autoimmune injury. Gastroenterology 120, 1485–1501.
Kobayashi, E., Kobayashi, M., Tsuneyama, K., Fukami, T., Nakajima, M., Yokoi, T., 2009. Halothane-induced liver injury is mediated by interleukin-17 in mice. Toxicol. Sci. 111, 302–310.
Kostenis, E., Ulven, T., 2006. Emerging roles of DP and CRTh2 in allergic inflammation. Trends Mol. Med. 12, 148–158.
Kumada, T., Tsuneyama, K., Hatta, H., Ishizawa, S., Takano, Y., 2004. Improved 1-h rapid immunostaining method using intermittent microwave irradiation: practicability based on 5 years application in Toyama Medical and Pharmaceutical University Hospital. Mod. Pathol. 17, 1141–1149.
Leonard, W.J., O'Shea, J.J., 1998. Jaks and STATs: biological implications. Annu. Rev. Immunol. 16, 293–322.
Maddox, J.F., Domzalski, A.C., Roth, R.A., Ganey, P.E., 2004. 15-Deoxy prostaglandin J_2 enhances allyl alcohol-induced toxicity in rat hepatocytes. Toxicol. Sci. 77, 290–298.
Nelms, K., Keegan, A.D., Zamorano, J., Ryan, J.J., Paul, W.E., 1999. The IL-4 receptor: signaling mechanisms biologic functions. Annu. Rev. Immunol. 17, 701–738.
Njoku, D.B., Li, Z., Washington, N.D., Mellerson, J.L., Talor, M.V., Sharma, R., Rose, N.R., 2009. Suppressive and pro-inflammatory roles for IL-4 in the pathogenesis of experimental drug-induced liver injury. Eur. J. Immunol. 39, 1652–1663.
Olsson, R., Wiholm, B.E., Sand, C., Zettergren, L., Hultcrantz, R., Myehed, M., 1992. Liver damage from flucloxacillin, cloxacillin, dicloxacillin. J. Hepatol. 15, 154–161.
Palmer, C.D., Restifo, P.N., 2009. Suppressors of cytokine signaling (SOCS) in T cell differentiation, maturation, and function. Trends Immunol. 30, 592–602.
Reilly, T.P., Brady, J.N., Marchick, M.R., Bourdi, M., George, J.W., Radonovich, M.F., Pise-Masison, C.A., Pohl, L.R., 2001. A protective role for cyclooxygenase-2 in drug-induced liver injury in mice. Chem. Res. Toxicol. 14, 1620–1628.
Shaw, P.J., Ditewig, A.C., Waring, J.F., Liguori, M.J., Blomme, E.A., Ganey, P.E., Roth, R.A., 2009. Coexposure of mice to trovafloxacin and lipopolysaccharide, a model of idiosyncratic hepatotoxicity, results in a unique gene expression profile and interferon gamma-dependent liver injury. Toxicol. Sci. 107, 270–280.
Spanakis, N.E., Garinis, G.A., Alexopoulos, E.C., Patrinos, G.P., Menounos, P.G., Sklavounou, A., Manolis, N.E., Gorgoulis, V.G., Valis, D., 2002. Cytokines serum levels in patients with chronic HCV infection. J. Clin. Lab. Anal. 16, 40–46.
Spik, I., Brenuchon, C., Angeli, V., Staumont, D., Fleury, S., Capron, M., Trottein, F., Dombrowicz, D., 2005. Activation of the prostaglandin D_2 receptor DP2/CRTH2 increases allergic inflammation in mouse. J. Immunol. 174, 3703–3708.
Stein, G.E., 2005. Safety of newer parenteral antibiotics. Clin. Infect. Dis. 41, 293–302.
Steinman, L., 2007. A brief history of Th17, the first major revision in the Th1/Th2 hypothesis if T cell-mediated tissue damage. Nat. Rev. Med. 13, 139–145.
Takeshita, K., Yamasaki, T., Nagano, K., Sugimoto, H., Shichijo, M., Gantner, F., Bacon, B.K., 2004. CRTH2 is a prominent effector in contact hypersensitivity-induced neutrophil inflammation. Int. Immunol. 16, 947–959.
Zou, W., Devi, S.S., Sparkenbaugh, E., Younis, H.S., Roth, R.A., Ganey, P.E., 2009. Hepatotoxic interaction of sulindac with lipopolysaccharide: role of the hemostatic system. Toxicol. Sci. 108, 184–193.

Drug Metab. Pharmacokinet. 26 (3): 256–265 (2011).

Regular Article

Interpretation of the Effects of Protein Kinase C Inhibitors on Human UDP-glucuronosyltransferase 1A (UGT1A) Proteins *in cellulo*

Yuko ABE, Ryoichi FUJIWARA, Shingo ODA, Tsuyoshi YOKOI and Miki NAKAJIMA*

Drug Metabolism and Toxicology, Faculty of Pharmaceutical Sciences, Kanazawa University, Kanazawa, Japan

Full text of this paper is available at http://www.jstage.jst.go.jp/browse/dmpk

Summary: UDP-glucuronosyltransferases (UGTs) catalyze the glucuronidation of a wide variety of xeno/endobiotics. Previous studies have reported that human UGT enzymes are phosphorylated and that treatment of cells with protein kinase C (PKC) inhibitors results in decreased UGT activities without affecting the UGT protein levels. In this study, we investigated the effects of PKC inhibitors on human UGT1A protein levels and activities in detail. When UGT1A-expressing HEK293 cells and LS180 cells were treated with curcumin or calphostin C, the exogenous and endogenous UGT1A protein levels in homogenates prepared with Tris-buffered saline were significantly decreased. Enzyme activity levels mirrored the changes in UGT protein levels. When the curcumin- or calphostin C-treated cells were lysed with buffer containing a detergent, the UGT protein levels did not decrease. We found that curcumin or calphostin C treatment facilitated the degradation of UGT protein after the cells were collected in the absence of a detergent. Finally, by *in cellulo* evaluation, we found that curcumin decreased UGT activity by the direct inhibitory effect, but calphostin C did not affect UGT activity. Thus, this study suggests that we should evaluate the data carefully when interpreting the effects of PKC inhibitors on UGT activity.

Keywords: UGT; glucuronidation; phosphorylation; degradation; inhibition

Introduction

UDP-glucuronosyltransferases (UGTs; EC 2.4.1.17) are a superfamily of enzymes that catalyze the conjugation of endogenous and exogenous compounds with UDP-glucuronic acid (UDPGA) as a cosubstrate.[1] UGT enzymes are localized to the endoplasmic reticulum membrane. The transmembrane domain is near the carboxyl terminus and most of the mass is on the luminal side.[2] Human UGTs are subdivided into two families, UGT1 and UGT2, based on amino acid sequence identity. To date, 19 individual UGT isoforms have been identified in humans.[3] These isoforms have different or overlapping substrate specificities and show tissue-specific expressions.

Protein phosphorylation is one of the most common protein modifications. Previous studies have reported that the phosphorylation event affects UGT activity: Basu *et al.*[4] first reported that the treatment of LS180 cells, HT-29 cells, or UGT1A1-expressing COS-1 cells with curcumin and calphostin C, which are potent inhibitors of protein kinase C (PKC), decreased glucuronosyltransferase activities toward bilirubin and anthraflavic acid without affecting UGT protein levels. They demonstrated that UGT1A1 incorporated [^{33}P]orthophosphate, which was inhibited by calphostin C. Mutations in predicted phosphorylation sites of UGT1A1 (T75A, T112A, and S435G) resulted in decreased enzyme activities. In 2004, Basu *et al.* found similar results for human UGT1A10, which is expressed in the gastrointestinal tract.[5] Subsequently, they reported that overexpression or inhibition of PKCε, as well as mutation of the predicted phosphorylation sites, altered the substrate preference of UGT1A7.[6] In 2008, they reported that treatment of LS180 cells with calyculin A, a phosphatase inhibitor I, or PKC agonists such as 1,2-dihexanoyl-*sn*-glycerol, facilitated restoration of UGT activity.[7]

In this study, we examined the effects of curcumin and calphostin C on the activities and protein levels of UGTs *in vitro* and *in cellulo*. We treated UGT1A1-, UGT1A4-, UGT1A6-, UGT1A7-, and UGT1A9-expressing HEK293 cells and LS180 cells, which endogenously express UGT enzymes, with curcumin and calphostin C. We found a significant inconsistency between the previous studies and our current work, and noted that we should evaluate the data carefully when interpreting the effects of PKC inhibitors on UGT activity.

Received; December 10, 2010, Accepted; January 28, 2011
J-STAGE Advance Published Date: February 8, 2011, doi:10.2133/dmpk.DMPK-10-RG-121
**To whom correspondence should be addressed:* Miki NAKAJIMA, Ph.D., *Drug Metabolism and Toxicology, Faculty of Pharmaceutical Sciences, Kanazawa University, Kanazawa 920-1192, Japan. Tel. +81-76-234-4407, Fax. +81-76-234-4407, E-mail: nmiki@p.kanazawa-u.ac.jp*

Materials and Methods

Chemicals and reagents: UDPGA, alamethicin, 4-methylumbelliferone (4-MU), leflunomide, MG-132, and wortmannin were purchased from Sigma-Aldrich (St. Louis, MO). Curcumin, calphostin C, and genistein were purchased from Wako Pure Chemicals (Osaka, Japan). Caspase inhibitor I and calpain inhibitor *N*-acetyl-leucyl-leucyl-norleucinal (ALLN) were purchased from Merck (Darmstadt, Germany). Rabbit anti-human UGT1A polyclonal antibody was obtained from BD Gentest (Woburn, MA). Mouse anti-KDEL monoclonal antibody was obtained from Stressgen (Victoria, Canada). Rabbit anti-human GAPDH antibody was purchased from Imgenex (San Diego, CA).

Cells culture and chemical treatment: HEK293 cells stably expressing human UGT1A1, UGT1A4, UGT1A6, and UGT1A9 were established previously.[8] HEK293 cells stably expressing human UGT1A7 was established by the transfection of an expression vector containing UGT1A7 cDNA.[9] These cells were cultured in Dulbecco's modified Eagle's medium (DMEM) supplemented with 4.5 g/L glucose, 10 mM HEPES, and 10% fetal bovine serum (FBS) (Invitrogen, Carlsbad, CA). LS180 cells were obtained from the American Type Culture Collection (Rockville, MD) and cultured in DMEM supplemented with 10% FBS and 0.1 mM nonessential amino acids (Invitrogen). HEK293 cells and LS180 cells were maintained at 37°C under an atmosphere of 5% CO_2–95% air. The cells were treated with curcumin, calphostin C, genistein, or leflunomide. To inhibit protein degradation systems, the cells were treated with MG-132, wortmannin, chloroquine, ALLN, or caspase inhibitor I for 1 h before the treatment with curcumin or calphostin C. These chemicals, except for chloroquine (which was dissolved in water), were dissolved in dimethyl sulfoxide with a final concentration in the medium of less than 0.2%.

Preparation of cell homogenate: Cells were suspended in Tris-buffered saline (TBS) [25 mM Tris-HCl buffer (pH 7.4), 138 mM NaCl, and 2.7 mM KCl] and disrupted by freeze-thawing three times as described previously.[8] The suspensions were homogenized by 10 strokes with a Teflon-glass homogenizer. In some cases, the cells were lysed with 0.2% sodium dodecyl sulfate (SDS) or 1% Triton X-100 in TBS. The protein concentrations were determined by Bradford assay.[10]

Immunoblot analysis: UGT protein levels were determined by SDS-polyacrylamide gel electrophoresis (SDS-PAGE) and immunoblotting. Cell homogenates from HEK293 cells and LS180 cells, prepared as described above, were boiled for 3 min in Laemmli sample buffer containing 2-mercaptoethanol. A total of 10 μg (HEK293 cells) or 50 μg (LS180 cells) of proteins were separated on a 10% polyacrylamide gel[11] and transferred onto a polyvinylidene difluoride membrane (Immobilon-P, Millipore, Bedford, MA). The membrane was blocked in 3% nonfat dry milk in phosphate-buffered saline (PBS) containing 0.1% Tween 20 at room temperature for 3 h. The membrane was incubated with rabbit anti-human UGT1A polyclonal antibody (1:500, PBS) overnight at room temperature. Biotinylated anti-rabbit IgG and a VECTSTAIN ABC kit (Vector Laboratories, Burlingame, CA) were used for diaminobenzidine staining.

Reverse transcriptase-polymerase chain reaction analysis: Total RNA was extracted from HEK293 cells expressing UGT1A9 or LS180 cells using ISOGEN (Nippon Gene, Tokyo, Japan). Reverse transcriptase-polymerase chain reaction (RT-PCR) analyses for UGT1A9, UGT1A1, and glyceraldehyde-3-phosphate dehydrogenase (GAPDH) were performed as described previously.[12] The PCR products (15 μl) were analyzed by electrophoresis with 2% agarose gel and visualized by ethidium bromide staining.

Enzyme assays: 4-MU *O*-glucuronide formation was determined as described previously[8] with slight modifications. Briefly, a typical incubation mixture (200 μl total volume) contained 50 mM Tris-HCl buffer (pH 7.4), 10 mM $MgCl_2$, 2.5 mM UDPGA, 25 μg/ml alamethicin, 0.1 mg/ml total cell homogenate, and 10 μM 4-MU. The reaction was initiated by the addition of UDPGA after a 3-min preincubation at 37°C. After incubation at 37°C for 15 min, the reaction was terminated by the addition of 100 μl of cold methanol. After removal of the protein by centrifugation at 13,000*g* for 5 min, a 20-μl portion of the sample was subjected to HPLC. The HPLC apparatus and conditions were described previously.[8]

For the inhibition study, the concentrations of 4-MU and curcumin ranged from 1–40 μM and 0.05–0.5 μM, respectively. Dixon plots were used for the determination of the type of inhibition. Kinetic parameters were determined by nonlinear regression analysis using appropriate software (K-cat, BioMetallics, Princeton, NJ).

For the *in cellulo* glucuronidation assay, cells were incubated with culture medium containing 10 μM 4-MU for 2 h at 37°C. After incubation, a 200-μl portion of the medium was collected and extracted with an equal volume of chloroform. After centrifugation at 13,000*g* for 5 min, a 20-μl portion of the supernatant was subjected to HPLC.

Determination of curcumin concentration in culture media: After curcumin was added at a final concentration of 30 μM, a 100-μl portion of medium was collected at various times. To the media, 4 volumes of acetonitrile were added and vigorously mixed. After centrifugation at 15,000*g* for 5 min, the supernatant was subjected to HPLC. HPLC was performed using an L-7100 pump (Hitachi, Tokyo, Japan), an L-7485 FL detector (Hitachi), an L-7200 autosampler (Hitachi), a D-2500 integrator (Hitachi), and a Symmetry column (4.6 mm × 150 mm, 5 μm; Waters, Milford, MA). The flow rate was 1 mL/min and the column temperature was 35°C. Detection was accomplished with a florescence detector

at 420-nm excitation and 540-nm emission. The mobile phase was 40% acetonitrile adjusted to pH 3.0 with formic acid.

Immunoprecipitation assay: Anti-UGT1AC antibody,[13] an antibody against the common C-terminal region of UGT1A protein, was a generous gift from Dr. Shin-ichi Ikushiro (Toyama Prefectural University, Toyama, Japan). HEK293 cells expressing UGT1A9 cells were treated with curcumin or calphostin C for 1 h and lysed with a buffer containing 1% triton X-100, 0.2% SDS, and 2 mM EDTA. Immunoprecipitation was performed using anti-UGT1AC antibody as described previously,[8] and the immunoprecipitates were subjected to immunoblot analysis using anti-UGT1A, anti-phosphoserine, anti-phosphothreonine, or anti-phosphotyrosine antibodies (ZYMED Laboratories, San Francisco, CA).

Pro-Q Diamond phosphoprotein staining of purified His-tagged UGT1A9: A pFastBac plasmid containing histidine (His)-tagged UGT1A9 cDNA[14] was kindly provided by Dr. Moshe Finel (University of Helsinki, Helsinki, Finland). The recombinant baculovirus was infected to insect cells, and the produced His-tagged UGT1A9 was purified using Ni-NTA Agarose (Qiagen, Hilden, Germany) as described previously.[14] The purified protein was subjected to staining using a Pro-Q Diamond phosphoprotein gel stain kit (Invitrogen). Silver staining and immunoblot analysis using anti-His antibody (Qiagen) were also performed to confirm the purification.

Results

Curcumin and calphostin C decrease UGT protein levels: HEK293 cells expressing human UGT1A1 were treated with curcumin or calphostin C for 1 h, and cell homogenates were prepared using TBS. On immunoblot analysis, we found that UGT1A1 protein levels were dramatically decreased by treatment with curcumin and with calphostin C in a dose-dependent manner (**Fig. 1A**). The same phenomenon was observed for UGT1A4, UGT1A6, UGT1A7, and UGT1A9. In contrast, the expression levels of glucose regulated protein (GRP) 94 and GRP78, which are localized in the endoplasmic reticulum membrane like UGTs, and GAPDH were not affected. These results suggested that curcumin and calphostin C specifically decreased the UGT1A protein levels. Calphostin C is a specific inhibitor of PKC, whereas curcumin inhibits tyrosine kinase as well as PKC.[15] Therefore, we investigated the effects of tyrosine kinase inhibitors on UGT1A protein levels. Treatment with genistein or leflunomide for 1 h did not affect UGT1A protein levels.

LS180 cells were used to investigate the effects on endogenous UGT1A proteins (**Fig. 1B**). Since multiple UGT1A isoforms are expressed in LS180 cells, we evaluated the overall protein level of UGT1As using anti-UGT1A antibody. We found that UGT1A protein levels decreased on treatment with curcumin or calphostin C in a dose-dependent manner (**Fig. 1B**), but GRP94, GRP78, and GAPDH protein levels did not decrease. Also, tyrosine kinase inhibitors did not affect UGT1A protein levels. These results suggest that curcumin and calphostin C specifically decrease UGT1A protein levels irrespective of the isoforms or exogenous or endogenous protein expression.

Curcumin and calphostin C do not affect UGT1A mRNA levels: We investigated whether UGT1A mRNA levels are affected by treatment with curcumin or calphostin C (**Fig. 2**). RT-PCR analysis revealed that UGT1A9 mRNA levels in the HEK293 expression system (**Fig. 2A**) and UGT1A1 mRNA levels in LS180 cells (**Fig. 2B**) were not affected by treatment with curcumin or calphostin C. These results suggest that the decrease of UGT1A protein levels by curcumin or calphostin C treatment was not caused by the suppression of transcription.

Effects of curcumin or calphostin C on UGT1A protein varies with the treatment time: We examined UGT1A protein levels as well as UGT1A activity after treatment with 30 μM curcumin or 100 nM calphostin C for various times (1 min, 0.25, 0.5, 1, 2, 6, 12, and 24 h). When HEK293 cells expressing UGT1A9 were treated with curcumin, the UGT1A9 protein level fell below the detection limit after only a 1-min incubation (**Fig. 3A**). The loss of UGT1A9 protein continued up to 12 h of incubation. Interestingly, the UGT1A9 protein level slightly recovered on 24-h treatment. When the cells were treated with calphostin C, the UGT1A9 protein level fell to 60% of the control with a 1-min treatment, and gradually decreased in a time-dependent manner until 24 h. When LS180 cells were treated with curcumin, the UGT1A protein level fell to 5% of control on a 1-min treatment (**Fig. 3A**). After 15 min of treatment, the UGT1A protein level fell below the detection limit. This reduction continued up to 2 h of treatment. The UGT1A protein level was markedly restored (60–100% of control) when the cells were treated for 6–24 h. When the cells were treated with calphostin C, the UGT1A protein level fell to 50% of the control with a 1-min treatment, and gradually decreased in a time-dependent manner until 24 h. 4-MU *O*-glucuronosyltransferase activities of total cell homogenates prepared from HEK293 cells and from LS180 cells were modified by treatment with curcumin and calphostin C in parallel with changes in UGT1A protein levels (**Fig. 3B**).

Concerning the restoration of the UGT protein level after longer incubation periods with curcumin, we surmised that the concentration of curcumin in the media might decrease during the culture because it has been reported that curcumin is metabolized by UGTs.[16] As shown in **Figure 3C**, we found that the concentration of curcumin in the HEK293 cell medium fell to 60% of control after 6 h of incubation, and gradually decreased thereafter (46% and 16% of control at 12- and 24-h incubations). The fall in concentration of curcumin in the LS180 cell medium was faster than that in the HEK293 cell medium. These results

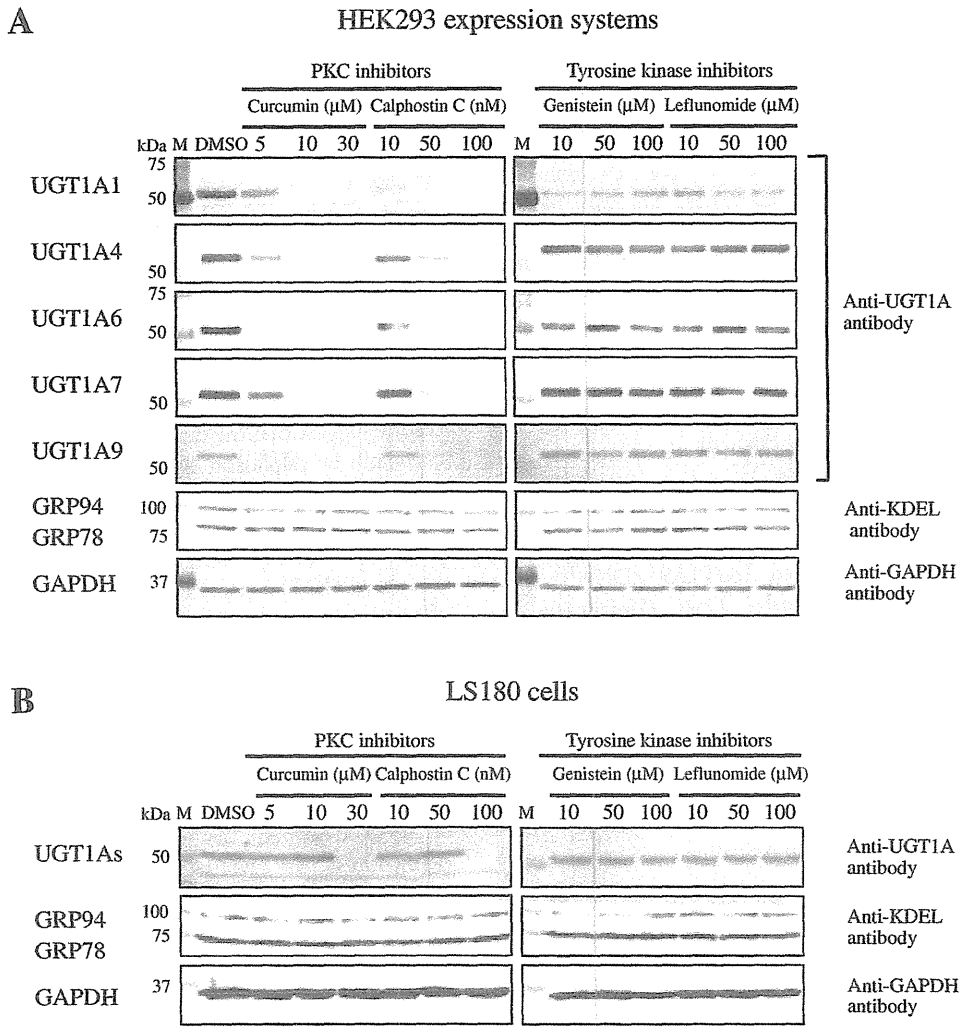

Fig. 1. Effects of PKC inhibitors and tyrosine kinase inhibitors on UGT1A protein levels
HEK293 cells expressing UGT1A1, UGT1A4, UGT1A6, UGT1A7, and UGT1A9 (A) and LS180 cells (B) were treated with curcumin, calphostin C, genistein, or leflunomide. After 1-h treatments, the cells were suspended in TBS and cell homogenates were prepared as described in Materials and Methods. Immunoblot analysis was performed using anti-UGT1A, anti-KDEL, and anti-GAPDH antibodies. M, marker.

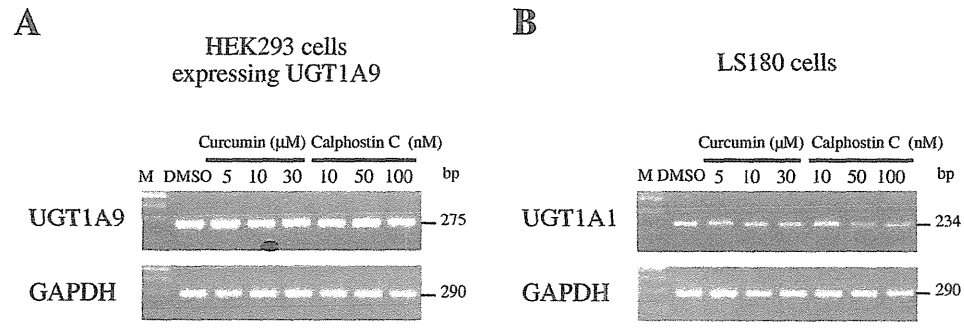

Fig. 2. Effects of curcumin and calphostin C on UGT1A9 mRNA in HEK293 cells and UGT1A1 mRNA in LS180 cells
Total RNA was extracted from cells treated with curcumin or calphostin C for 1 h. RT-PCR analysis was performed for UGT1A9 or UGT1A1 as well as GAPDH. M, marker.

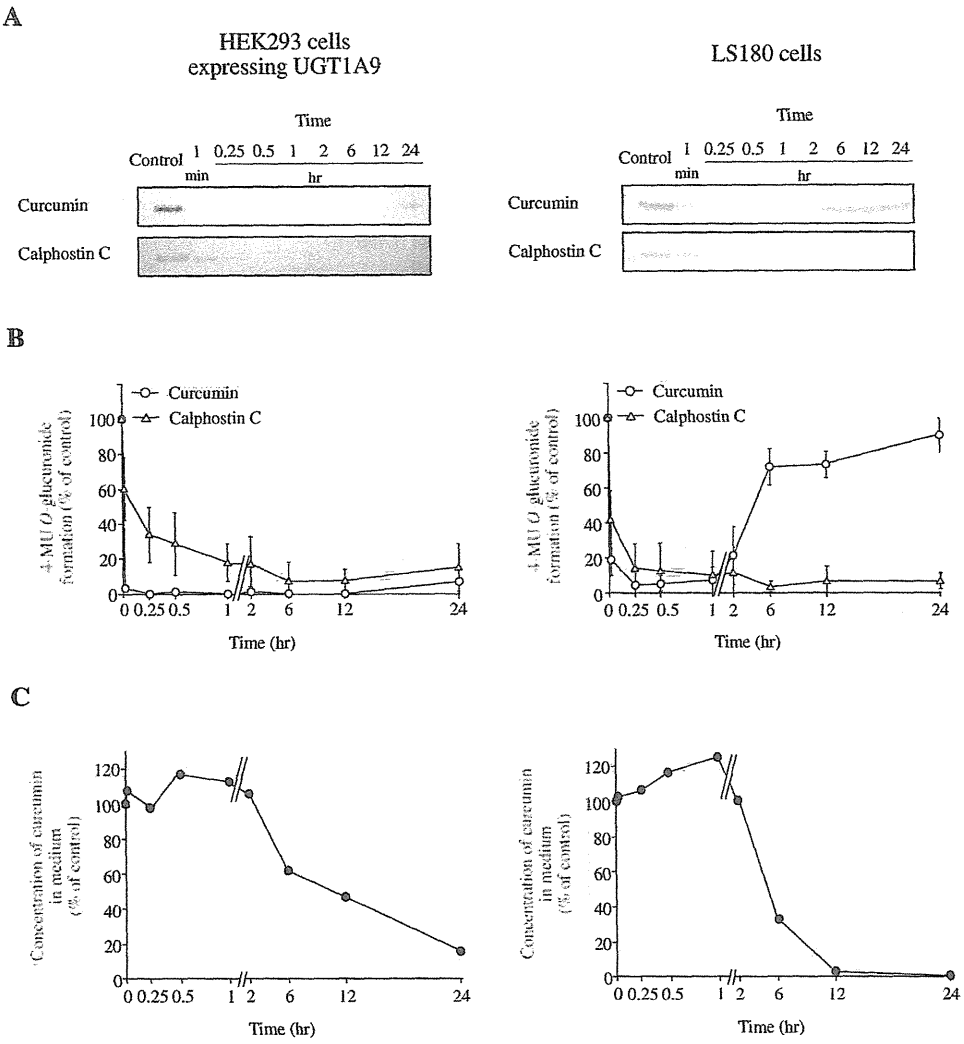

Fig. 3. Effects of curcumin and calphostin C on UGT1A proteins (A) and activities (B) in HEK293 cells and LS180 cells, and remaining curcumin concentrations in the medium (C)

HEK293 cells expressing UGT1A9 and LS180 cells were treated with 30 μM curcumin or 100 nM calphostin C for 1 min, 0.25, 0.5, 1, 2, 6, 12, or 24 h. Total cell homogenates were prepared and subjected to SDS-PAGE followed by immunoblot analysis with anti-UGT1A antibody (A). Using total cell homogenates, 4-MU *O*-glucuronosyltransferase activity was determined. The control activities of the total cell homogenates from HEK293 cells stably expressing UGT1A9 and LS180 cells were 4.3 nmol/min/mg protein and 0.9 nmol/min/mg protein, respectively (B). The remaining curcumin concentration in the cell culture medium was also determined by HPLC after the addition (time 0) of curcumin at a final concentration of 30 μM (C).

suggest that the restoration of UGT proteins was caused by the decrease of curcumin levels in the medium.

Proteasomes, autophagy, and protease inhibitors did not inhibit the loss of UGT1A9 protein: We suspected that the decrease of UGT1A protein on treatment with curcumin or calphostin C might be due to the acceleration of protein degradation. Proteasomes, autophagy, and proteases are major contributing factors of protein degradation. We treated HEK293 cells expressing UGT1A9 with inhibitors of proteasomes (MG-132), autophagy (chloroquine and wortmannin), and proteases (calpain inhibitor ALLN and caspase inhibitor I) for 2 h, and then treated the cells with 30 μM curcumin or 100 nM calphostin C for the last 1 h. However, these inhibitors did not stop the reduction of UGT1A9 protein levels by curcumin or calphostin C (**Fig. 4**). Additionally, we investigated the effects of other protease inhibitors such as *p*-amidinophenylmethanesulfonyl fluoride, trypsin inhibitor, leupeptin, aprotinin, and bestatin on the reduction of UGT1A9 protein levels; however, none of them could inhibit the degradation of UGT1A9 protein (data not shown). This data indicates that the reduction of UGT1A9 protein levels by curcumin or calphostin C was not mediated by proteasomes, autophagy, or proteases.

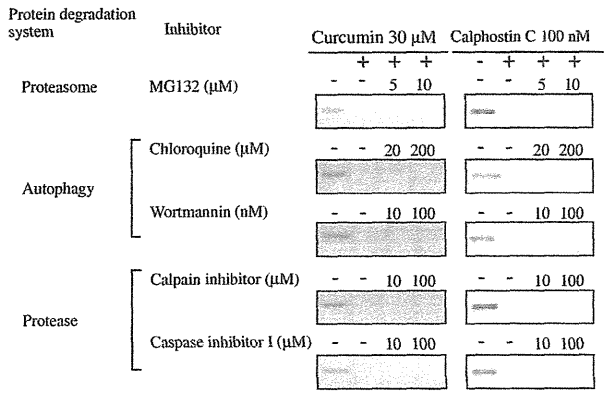

Fig. 4. Effects of proteasome, autophagy, and protease inhibitors on the degradation of UGT1A9 in curcumin- or calphostin C-treated HEK293 cells

After HEK293 cells expressing UGT1A9 were treated with MG132, chloroquine, wortmannin, calpain inhibitor, and caspase inhibitor I for 1 h, the cells were treated with curcumin or calphostin C for 1 h in the presence of these inhibitors. Total cell homogenates were prepared and subjected to SDS-PAGE followed by immunoblot analysis with anti-UGT1A antibody.

The loss of UGT1A protein by curcumin and calphostin C was not observed when the cells were collected with buffer containing a detergent: It was a surprising finding that UGT1A protein levels fell after only 1 min of treatment with curcumin (Fig. 3A). After the treatment, we collected the cells with TBS and prepared total cell homogenates by a conventional method for UGT studies. It takes approximately 2 h to finish the preparation of the cell homogenates. We surmised that UGT1A protein might be degraded during the preparation of the cell homogenates. To examine this hypothesis, we directly suspended the cells with Laemmli sample buffer containing 1.5% SDS[11] after treatment with curcumin for 1 h. When the cell lysate was used for the immunoblot analysis, the fall in UGT1A protein levels on curcumin treatment was not observed (Fig. 5A). We confirmed that UGT1A protein levels were not decreased by curcumin when the treated cells were suspended with 0.2% SDS or 1% Triton X-100. These results suggest that the degradation of UGT1A proteins by curcumin occurs after the collection of the treated cells.

Next, we sought to investigate when UGT1A protein starts to degrade after the collection of curcumin-treated cells. HEK293 cells expressing UGT1A9 or LS180 cells were treated with 30 μM curcumin for 1 h. Then, the cells were washed and collected with TBS and kept on ice. Just after the collection or 15, 30 min, 1, and 2 h after incubation on ice, the Laemmli sample buffer was added. By the immunoblot analysis of these samples, it was demonstrated that UGT1A9 in HEK293 cells and UGT1As in LS180 cells started to decrease after 1 h on ice (Fig. 5B). These results indicate that degradation of the UGT protein by curcumin occurs after the cells are collected. In addition, when the cell homogenates were incubated with curcumin and calphostin C, we didn't see any change of UGT protein levels (data not shown). Therefore, it was indicated that the degradation of UGT occurs only in cells treated with PKC inhibitors.

Effects of curcumin or calphostin C on UGT1A proteins and activities *in cellulo*: As shown in Figure 3, we investigated the time-dependency of the effects of curcumin and calphostin C on the UGT1A protein. However, the data should be carefully interpreted, because it was found that the change in the UGT1A protein levels occurred after the cells were collected. To understand the actual effects of curcumin and calphostin C on UGT1A protein levels, we performed immunoblot analysis using cell lysates directly prepared with the Laemmli sample buffer. We found that UGT1A9 levels in HEK293 cells and levels of UGT1As in LS180 cells were not changed (Fig. 6A). Next, we evaluated UGT activities *in cellulo* by adding a substrate to the medium and measuring the metabolite formed in the medium, because the cell lysates using the Laemmli sample

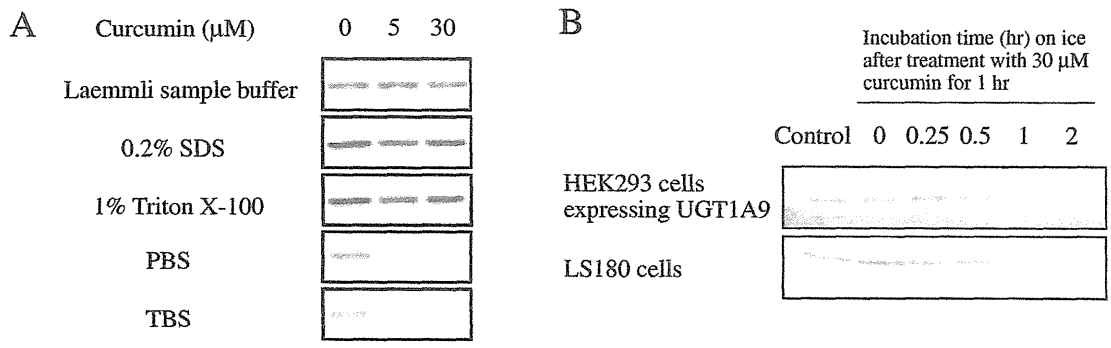

Fig. 5. Degradation of UGT in curcumin- or calphostin C-treated cells did not occur when the cells were collected with a buffer containing a detergent

HEK293 cells expressing UGT1A9 were treated with curcumin for 1 h. The cells were collected with Laemmli sample buffer, 0.2% SDS, 1% Triton X-100, PBS, or TBS, and subjected to SDS-PAGE followed by immunoblot analysis with anti-UGT1A antibody (A). The curcumin-treated HEK293 cells were washed and collected with TBS and kept on ice. Just after the collection (time 0), 0.25, 0.5, 1, or 2 h after the incubation on ice, the Laemmli sample buffer was added and immunoblot analysis was performed with anti-UGT1A antibody (B).

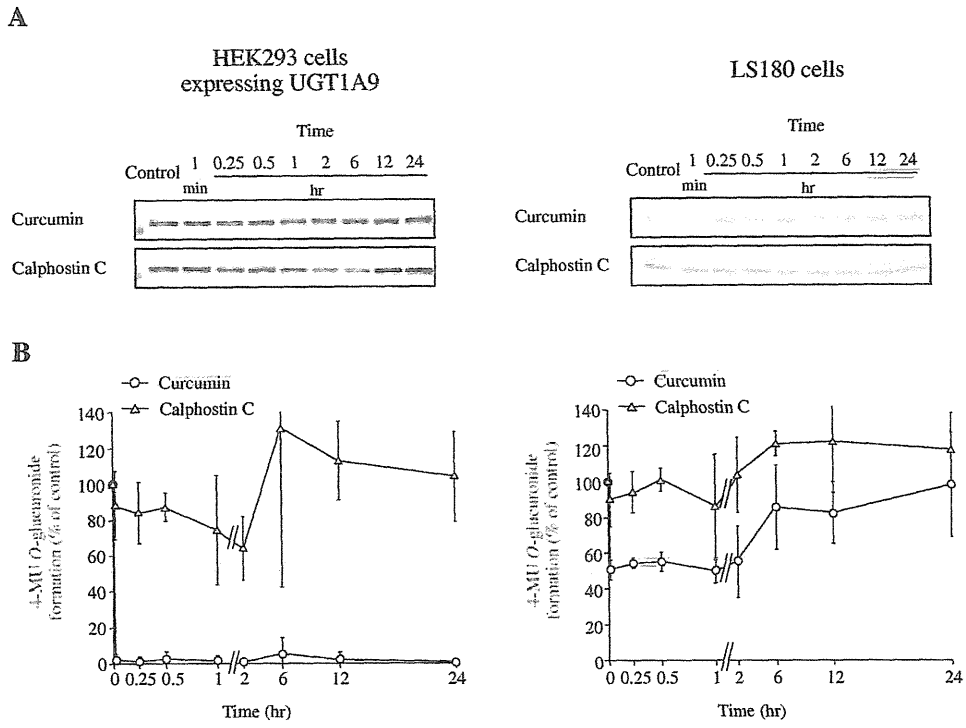

Fig. 6. UGT1A protein levels (A) and activities (B) evaluated *in cellulo* after treatment of the cells with curcumin or calphostin C
HEK293 cells expressing UGT1A9 and LS180 cells were treated with 30 μM curcumin or 100 nM calphostin C for 1 min, 0.25, 0.5, 1, 2, 6, 12, or 24 h. Cells were lysed with Laemmli sample buffer and immunoblot analysis was performed with anti-UGT1A antibody (A). UGT activities in the curcumin- or calphostin C-treated cells were evaluated *in cellulo*. 4-MU was added to the cell culture medium at a final concentration of 10 μM. After 2 h of incubation, the amount of 4-MU *O*-glucuronide in the medium was measured by HPLC (B). Data are mean ± SD (n = 3).

buffer could not be used for measurement of the enzyme activity. When the HEK293 and LS180 cells were treated with calphostin C, no significant change was observed in 4-MU *O*-glucuronide formation (Fig. 6B). In contrast, the 4-MU *O*-glucuronide formation in HEK293 cells expressing UGT1A9 was dramatically decreased in the presence of curcumin, and that in LS180 cells was decreased by 50% of control (up to 2 h of treatment) and by 20% (6–12 h of treatment) in the presence of curcumin.

Curcumin inhibits UGT1A9 activity: Since curcumin is a substrate for UGT enzymes, we speculated that the decreases of UGT activities *in cellulo* might be due to inhibition by curcumin. We examined the inhibitory effects of curcumin on 4-MU *O*-glucuronosyltransferase activity by total cell homogenates prepared from HEK293 cells expressing UGT1A9. It was demonstrated that curcumin potently (Ki = 0.26 μM) inhibited UGT1A9 activity in a noncompetitive manner (Fig. 7). Thus, the reduction in 4-MU glucuronidation activities by curcumin *in cellulo* is likely due to the direct inhibitory potency of curcumin toward UGT1A9.

Immunoprecipitation assay with anti-UGT1A antibody followed by immunoblotting with anti-phosphoserine, anti-phosphothreonine, or anti-phosphotyrosine antibodies: To examine whether the degradation of UGT proteins by curcumin and by calphostin C treatment links with the decrease in the phosphorylation status of the UGT proteins, we carried out an immunoprecipitation assay (Fig. 8). Curcumin- or calphostin C-treated HEK293 cells expressing UGT1A9

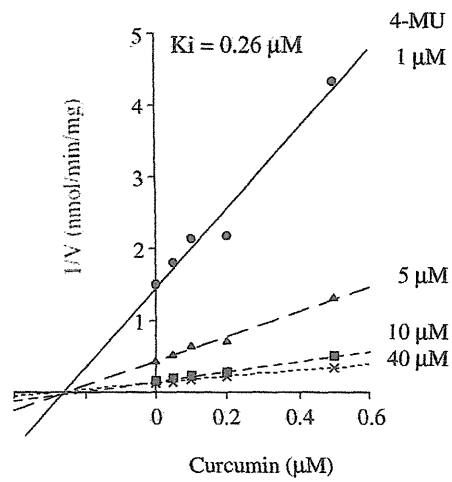

Fig. 7. Inhibitory effects of curcumin on 4-MU *O*-glucuronosyltransferase activity in cell homogenates from HEK293 cells expressing UGT1A9
The concentrations of 4-MU and curcumin were in the ranges 1–40 μM and 0.05–0.5 μM, respectively.

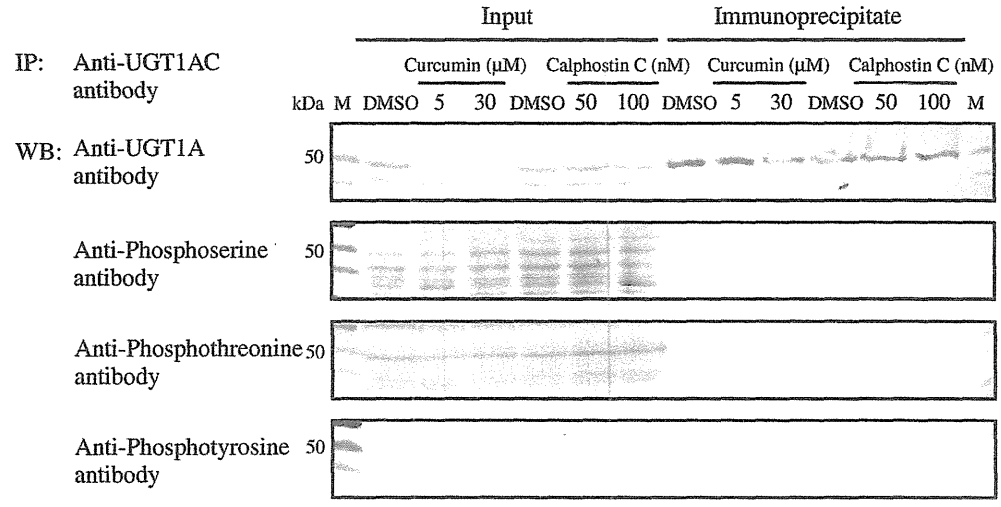

Fig. 8. Immunoprecipitation of UGT1A9 expressed in HEK293 cells and immunoblot analysis
HEK293 cells expressing UGT1A9 were treated with curcumin (5 or 30 μM) or calphostin C (50 or 100 nM) for 1 h. Cells were lysed with a buffer containing 1% Triton X-100, 0.2% SDS, and 2 mM EDTA and immunoprecipitation was performed using anti-human UGT1AC antibody. The immunoprecipitates were subjected to immunoblot analysis using anti-UGT1A, anti-phosphoserine, anti-phosphothreonine, or anti-phosphotyrosine antibodies. As controls, input proteins were also subjected to the immunoblot analysis. IP, immunoprecipitation; WB, Western blot; M, marker.

were lysed with a buffer containing 1% Triton X-100, 0.2% SDS, and 2 mM EDTA and subjected to immunoprecipitation using anti-UGT1AC antibody followed by immunoblotting with anti-UGT1A, anti-phosphoserine, anti-phosphothreonine, or anti-phosphotyrosine antibodies. UGT1A9 protein was successfully immunoprecipitated, but no phosphorylated UGT protein was detected. Thus, this experiment could not prove that UGT1A9 is phosphorylated. In addition, in the input protein, no obvious change was observed in the band pattern of phosphoprotein on curcumin or calphostin C treatment.

Pro-Q Diamond phosphoprotein staining of purified His-tagged UGT1A9: To further investigate whether UGT1A9 is phosphorylated, we carried out Pro-Q Diamond phosphoprotein staining of UGT1A9 protein. His-tagged UGT1A9 was purified using Ni-NTA Agarose and subjected to SDS-PAGE and silver staining, Pro-Q Diamond phosphoprotein staining, or immunoblot analysis with anti-His antibody. As shown in Figure 9, a band corresponding to His-tagged UGT1A9 was stained with the Pro-Q Diamond phosphoprotein gel stain kit, indicating that UGT1A9 protein was phosphorylated. However, in this experiment, we could not examine whether curcumin or calphostin C treatment had decreased the phosphorylation status because we prepared the membrane fraction with TBS, which causes degradation of UGT, before the purification step.

Discussion

Basu *et al.*[4–7] reported that the treatment of various cells expressing UGT with curcumin or calphostin C altered glucuronosyltransferase activities. They reported that these PKC inhibitors inhibited the incorporation of [^{33}P]orthophosphate into the UGT protein and decreased UGT activities without changing UGT protein levels. Furthermore, mutations at the predicted phosphorylation sites in UGTs resulted in decreased enzymatic activities. Based on these results, they concluded that the decreased activities were due to inhibition of the phosphorylation of the UGT enzymes. In contrast to their results, we found that UGT protein levels were dramatically decreased on treatment with curcumin or calphostin C (Figs. 1 and 3). To examine the reason for the inconsistency, we carefully read their papers and retrospectively noticed differences in the buffers used to prepare the homogenates. Basu *et al.*[4] used TBS, which is usually used for UGT analysis, for the preparation of homogenates to measure enzyme activities. However, for the preparation of cell lysates to perform immunoblot analysis, it seems that they used a buffer containing 1% Triton X-100 and 0.5% SDS.[17] First, we used TBS to prepare cell homogenates for immunoblot analysis and observed a decrease in UGT protein levels. In contrast, when we used buffer containing a detergent to lyse the cells, no decrease in UGT protein levels was observed on treatment with curcumin or calphostin C (Figs. 5 and 6). Thus, it should be emphasized that differences in the preparation method of cell homogenates may cause misinterpretation of the results. We concluded that decreased UGT activities on curcumin and calphostin C treatment were due to decreased UGT protein levels. Basu *et al.*[4] determined the effects of PKC inhibitors on UGT in LS180 and UGT-expressing COS-1 cells, and we determined those effects in LS180 and UGT-expressing HEK293 cells. In other words, the data from LS180 cells can be used as a

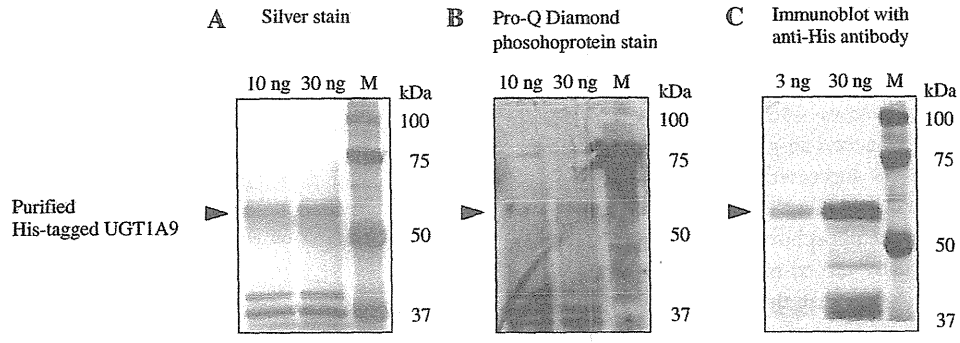

Fig. 9. Pro-Q Diamond phosphoprotein staining of purified His-tagged UGT1A9
Insect cells expressing His-tagged UGT1A9 were collected with TBS and a membrane fraction was prepared. The protein was purified using Ni-NTA Agarose and subjected to silver staining (A), Pro-Q Diamond phosphoprotein staining (B), or immunoblot analysis using anti-His antibody (C). M, marker.

reference between the two studies. Both studies found that the effects of PKC inhibitors were common to endogenous and exogenous UGTs. Therefore, we consider that the inconsistency was not due to the possibility that there are differences in signal transduction including the PKC system between the different cell lines.

To prepare cell homogenate, cells suspended in TBS were disrupted by freeze-thawing three times before homogenization. This is a common method for UGT analysis to elicit enzyme activity. One may question whether the freeze-thawing might possibly make UGT sensitive to PKC inhibitor-caused degradation. However, as shown in Figure 5B, when the curcumin-treated cells were lysed directly with Laemmli sample buffer without freeze-thawing, the degradation of UGT protein was still observed after the cells were kept on ice for 1 h. Thus, it is unlikely that freeze-thawing affected the degradation of UGT proteins resulting from treatment with PKC inhibitors. We found that UGT protein levels in the curcumin- or calphostin C-treated cells started to decrease 1 h after collection in the absence of detergents. We suspected that curcumin or calphostin C might facilitate the degradation of UGT proteins through proteasomes, autophagy, and proteases. However, we could not find evidence supporting this hypothesis (Fig. 4). Another possibility is that curcumin or calphostin C may decrease translation. However, since the machinery of translation is likely common for all proteins, the hypothesis would not explain the UGT-specific decrease. The underlying mechanism of the decrease of UGT protein levels by curcumin or calphostin C remains to be clarified.

To examine the actual effects of PKC inhibitors on UGT activities, we evaluated the activities *in cellulo*. Curcumin inhibited 4-MU *O*-glucuronidation activity by 50% at most in LS180 cells, but completely inhibited activity in HEK293 cells (Fig. 6B). We confirmed using cell homogenates from HEK293 cells expressing UGT1A9 that curcumin is a potent inhibitor of UGT1A9 (Fig. 7). Therefore, the inhibitory effects of curcumin on UGT activities seem to be independent of the inhibition of phosphorylation. LS180 cells express multiple UGT isoforms,[12] including UGT1A1 and UGT1A10, which showed high efficiency in terms of curcumin metabolism.[16] Thus, it is considered that the milder inhibitory effects of curcumin in LS180 cells compared to HEK293 cells could be due to the rapid elimination of curcumin in LS180 cells, as shown in Figure 3C. In contrast to curcumin, calphostin C did not affect UGT activity *in cellulo*. It has been reported that calphostin C treatment decreased [^{33}P]orthophosphate-labeled UGT1A protein levels.[4] Taken together, it seems that the phosphorylation status of UGT proteins does not significantly affect their enzymatic activities *in cellulo*. Although Basu *et al.*[4,5] reported that mutations at the predicted phosphorylation sites decreased UGT enzyme activities, the possibility that amino acid change *per se*, not the phosphorylation status, may change the enzyme activity cannot be excluded. To determine whether the UGT proteins are phosphorylated, we performed several experiments. An immunoprecipitation assay for UGT1A9 expressed in HEK293 cells using anti-UGT1AC antibody did not show the phosphorylation of UGT1A9 (Fig. 8). We also performed a Phos-tag SDS-PAGE analysis[18] using UGT1A9 expressed in HEK293 cells to investigate the phosphorylation status, but no evidence of phosphorylation was revealed (data not shown). Next, we performed Pro-Q Diamond phosphoprotein staining of purified His-tagged UGT1A9 and found that it was phosphorylated (Fig. 9). However, when the purified protein was subjected to LC-MS/MS analysis using a NanoFrontier eLD (Hitachi, Tokyo, Japan), no phosphorylated peptide was detected (data not shown). Therefore, a likely explanation is that, even if UGTs are originally phosphorylated, the extent of phosphorylation may not be so high.

During the process of preparing this report, another group reported the role of PKCδ in the functional activity of human UGT1A6.[19] They reported that rottlerin (a PKCδ selective inhibitor) and non-selective PKC inhibitors (calphostin C, curcumin, and hypericin) decreased acetamin-

ophen glucuronidation in LS180 cells by more than 50%. Although they did not observe an increase of serotonin glucuronidation in Sf9 cells expressing UGT1A6 on treatment with PKC activators such as phorbol myristate acetate and 1-oleoyl-2-acetyl-sn-glycerol, they found that co-expression of PKCδ increased the protein-normalized UGT1A6 activity in HEK293T cells. However, it remains to be examined whether the phosphorylation status of UGT1A6 was actually increased by the co-expression of PKCδ.

In conclusion, we found that the treatment of cells with curcumin and calphostin C resulted in a decrease of UGT protein levels. The degradation was observed only after the cells were collected with a buffer not containing a detergent. Even if the cells continued to be cultured in the presence of calphostin C, *in cellulo* UGT activity and protein levels were not affected. Thus, this study revealed that we should evaluate the data carefully when interpreting the effects of PKC inhibitors on UGT activity.

Acknowledgements: We thank Dr. Moshe Finel for providing the pFastBac plasmid containing His-tagged UGT1A9 cDNA and Dr. Shin-ichi Ikushiro for providing the anti-UGT1AC antibody. We acknowledge Mr. Brent Bell for reviewing the manuscript.

References

1) Dutton, G. J.: Acceptor substrates of UDP glucuronosyltransferase and their assay. In Dutton, G. J. (ed.): *Glucuronidation of Drugs and Other Compounds*, Boca Raton, FL, CRC Press, 1980, pp. 69–78.
2) Meech, R. and Mackenzie, P. I.: Structure and function of uridine diphosphate glucuronosyltransferases. *Clin. Exp. Pharmacol. Physiol.*, 24: 907–915 (1997).
3) Mackenzie, P. I., Bock, K. W., Burchell, B., Guillemette, C., Ikushiro, S., Iyanagi, T., Miners, J. O., Owens, I. S. and Nebert, D. W.: Nomenclature update for the mammalian UDP glycosyltransferase (UGT) gene superfamily. *Pharmacogenet. Genomics*, 15: 677–685 (2005).
4) Basu, N. K., Kole, L. and Owens, I. S.: Evidence for phosphorylation requirement for human bilirubin UDP-glucuronosyltransferase (UGT1A1) activity. *Biochem. Biophys. Res. Commun.*, 303: 98–104 (2003).
5) Basu, N. K., Kubota, S., Meselhy, M. R., Ciotti, M., Chowdhury, B., Hartori, M. and Owens, I. S.: Gastrointestinally distributed UDP-glucuronosyltransferase 1A10, which metabolizes estrogens and nonsteroidal anti-inflammatory drugs, depends upon phosphorylation. *J. Biol. Chem.*, 279: 28320–28329 (2004).
6) Basu, N. K., Kovarova, M., Garza, A., Kubota, S., Saha, T., Mitra, P. S., Banerjee, R., Rivera, J. and Owens, I. S.: Phosphorylation of a UDP-glucuronosyltransferase regulates substrate specificity. *Proc. Natl. Acad. Sci. USA*, 102: 6285–6290 (2005).
7) Basu, N. K., Kole, L., Basu, M., Chakraborty, K., Mitra, P. S. and Owens, I. S.: The major chemical-detoxifying system of UDP-glucuronosyltransferases requires regulated phosphorylation supported by protein kinase C. *J. Biol. Chem.*, 283: 23048–23061 (2008).
8) Fujiwara, R., Nakajima, M., Yamanaka, H., Nakamura, A., Katoh, M., Ikushiro, S., Sakaki, T. and Yokoi, T.: Effects of coexpression of UGT1A9 on enzymatic activities of human UGT1A isoforms. *Drug Metab. Dispos.*, 35: 747–757 (2007).
9) Izukawa, T., Nakajima, M., Fujiwara, R., Yamanaka, H., Fukami, T., Takamiya, M., Aoki, Y., Ikushiro, S., Sakaki, T. and Yokoi, T.: Quantitative analysis of UDP-glucuronosyltransferase (UGT) 1A and UGT2B expression levels in human livers. *Drug Metab. Dispos.*, 37: 1759–1768 (2009).
10) Bradford, M. M.: A rapid and sensitive method for the quantitation of microgram quantities of protein utilizing the principle of protein-dye binding. *Anal. Biochem.*, 72: 248–254 (1976).
11) Laemmli, U. K.: Cleavage of structural proteins during the assembly of the head of bacteriophage T4. *Nature*, 227: 680–685 (1970).
12) Nakamura, A., Nakajima, M., Yamanaka, H., Fujiwara, R. and Yokoi, T.: Expression of UGT1A and UGT2B mRNA in human normal tissues and various cell lines. *Drug Metab. Dispos.*, 36: 1461–1464 (2008).
13) Ikushiro, S., Emi, Y., Kato, Y., Yamada, S. and Sakaki, T.: Monospecific antipeptide antibodies against human hepatic UDP-glucuronosyltransferase 1A subfamily (UGT1A) isoforms. *Drug Metab. Pharmacokinet.*, 21: 70–74 (2006).
14) Kurkela, M., García-Horsman, J. A., Luukkanen, L., Mörsky, S., Taskinen, J., Baumann, M., Kostiainen, R., Hirvonen, J. and Finel, M.: Expression and characterization of recombinant human UDP-glucuronosyltransferases (UGTs). UGT1A9 is more resistant to detergent inhibition than other UGTs and was purified as an active dimeric enzyme. *J. Biol. Chem.*, 278: 3536–3544 (2003).
15) Hong, R. L., Spohn, W. H. and Hung, M. C.: Curcumin inhibits tyrosine kinase activity of p185neu and also depletes p185neu. *Clin. Cancer Res.*, 5: 1884–1891 (1999).
16) Hoehle, S. I., Pfeiffer, E. and Metzler, M.: Glucuronidation of curcuminoids by human microsomal and recombinant UDP-glucuronosyltransferases. *Mol. Nutr. Food Res.*, 51: 932–938 (2007).
17) Ritter, J. K., Yeatman, M. T., Kaiser, C., Gridelli, B. and Owens, I. S.: A phenylalanine codon deletion at the *UGT1* gene complex locus of a Crigler-Najjar type I patient generates a pH-sensitive bilirubin UDP-glucuronosyltransferase. *J. Biol. Chem.*, 268: 23573–23579 (1993).
18) Kinoshita, E., Kinoshita-Kikuta, E., Takiyama, K. and Koike, T.: Phosphate-binding tag, a new tool to visualize phosphorylated proteins. *Mol. Cell. Proteomics*, 5: 749–757 (2006).
19) Volak, L. P. and Court, M. H.: Role for protein kinase C delta in the functional activity of human UGT1A6: implications for drug-drug interactions between PKC inhibitors and UGT1A6. *Xenobiotica*, 40: 306–318 (2010).

0090-9556/11/3905-838–846$25.00
DRUG METABOLISM AND DISPOSITION
Vol. 39, No. 5
37259/3683405
Printed in U.S.A.

DMD 39:838–846, 2011

CYP2C9-Mediated Metabolic Activation of Losartan Detected by a Highly Sensitive Cell-Based Screening Assay[S]

Atsushi Iwamura, Tatsuki Fukami, Hiroko Hosomi, Miki Nakajima, and Tsuyoshi Yokoi

Drug Metabolism and Toxicology, Faculty of Pharmaceutical Sciences, Kanazawa University, Kanazawa, Japan

Received November 14, 2010; accepted February 14, 2011

ABSTRACT:

Drug-induced hepatotoxicity is a major problem in drug development, and reactive metabolites generated by cytochrome P450s are suggested to be one of the causes. CYP2C9 is one of the major enzymes in hepatic drug metabolism. In the present study, we developed a highly sensitive cell-based screening system for CYP2C9-mediated metabolic activation using an adenovirus vector expressing CYP2C9 (AdCYP2C9). Human hepatocarcinoma HepG2 cells infected with our constructed AdCYP2C9 for 2 days at multiplicity of infection 10 showed significantly higher diclofenac 4′-hydroxylase activity than human hepatocytes. AdCYP2C9-infected cells were treated with several hepatotoxic drugs, resulting in a significant increase in cytotoxicity by treatment with losartan, benzbromarone, and tienilic acid. Metabolic activation of losartan by CYP2C9 has never been reported, although the metabolic activations of benzbromarone and tienilic acid have been reported. To identify the reactive metabolites of losartan, the semicarbazide adducts of losartan were investigated by liquid chromatography-tandem mass spectrometry. Two CYP2C9-specific semicarbazide adducts of losartan (S1 and S2) were detected. S2 adduct formation suggested that a reactive metabolite was produced from the aldehyde metabolite E3179, but a possible metabolite from S1 adduct formation was not produced via E3179. In conclusion, a highly sensitive cell-based assay to evaluate CYP2C9-mediated metabolic activation was established, and we found for the first time that CYP2C9 is involved in the metabolic activation of losartan. This cell-based assay system would be useful for evaluating drug-induced cytotoxicity caused by human CYP2C9.

Introduction

Drug-induced hepatotoxicity is a serious problem in drug development and clinical practice. In the United States, it accounts for more than 50% of cases of acute liver failure, and more than 600 drugs have been associated with hepatotoxicity (Lee, 2003; Park et al., 2005). That is why some drugs that were launched on the market were later withdrawn. Therefore, the prediction of drug-induced hepatotoxicity before clinical trials is important in drug development, and multiple cell-based assays have been developed for evaluation of drug-induced hepatotoxicity (Greer et al., 2010). Sometimes, drug-induced hepatotoxicity is associated with reactive metabolites produced by drug-metabolizing enzymes (Guengerich, 2008). However, species differences in drug-metabolizing enzymes or other factors between humans and laboratory animals are a major problem in predicting the hepatotoxicity.

Cytochrome P450 (P450) enzymes are the most studied drug-metabolizing enzymes, accounting for ~75% of the metabolism of clinical drugs (Guengerich, 2008). Among them, CYP3A4 is the predominant isoform expressed in human liver, accounting for up to 60% of the total hepatic P450 protein and responsible for more than 50% of drug metabolism (Guengerich, 2008). To date, many researchers have tried to predict drug-induced hepatotoxicity in vitro using human hepatocarcinoma HepG2 cells, but the low expression levels of P450 enzymes in HepG2 cells may be responsible for the fact that 30% of the compounds were falsely classified as nontoxic (Rodríguez-Antona et al., 2002; Hewitt and Hewitt, 2004). Useful in vitro cell-based assays have been established with HepG2 cells, leading to improved evaluation of drug-induced cytotoxicity. For example, our previous study showed that benzodiazepines such as flunitrazepam and nimetazepam were metabolically activated by CYP3A4 by coincubation with HepG2 cells and CYP3A4 Supersomes (Mizuno et al., 2009). Vignati et al. (2005) demonstrated that various hepatotoxic drugs such as flutamide and troglitazone were activated by CYP3A4 using HepG2 cells transiently transfected with CYP3A4. Thus, the activation of hepatotoxic drugs by CYP3A4 has been well evaluated, but the contribution of other P450 enzymes remains to be evaluated. CYP2C is the second most highly expressed P450 subfamily in human liver, and CYP2C9 is the most highly expressed isoform in this family

This work was supported in part by Research on Advanced Medical Technology, Health and Labor Science Research from the Ministry of Health, Labor, and Welfare of Japan [Grant H20-BIO-G001].

Article, publication date, and citation information can be found at http://dmd.aspetjournals.org.

doi:10.1124/dmd.110.037259.

[S] The online version of this article (available at http://dmd.aspetjournals.org) contains supplemental material.

ABBREVIATIONS: P450, cytochrome P450; Nrf2, nuclear factor-E2 p-45-related factor; GFP, green fluorescent protein; GAPDH, glyceraldehyde-3-phosphate dehydrogenase; siRNA, small interfering RNA; HPLC, high-performance liquid chromatography; WST-8, 2-(2-methoxy-4-nitrophenyl)-3-(4-nitrophenyl)-5-(2, 4-disulfophenyl)-2*H*-tetrazolium monosodium salt; LC, liquid chromatography; MS/MS, tandem mass spectrometry; LCMS-IT-TOF, liquid chromatography ion trap time-of-flight mass spectrometry; MOI, multiplicity of infection; BSO, buthionine sulfoximine; ALT, alanine aminotransferase; FLU-1, 4-nitro-3-(trifluoromethyl)phenylamine.

(Edwards et al., 1998). CYP2C9 is responsible for the metabolism of various pharmaceutical drugs and appears to be partially involved in the generation of reactive metabolites, as is CYP3A4 (Li, 2002). For example, benzbromarone is metabolized via 6-hydroxybenzbromarone to a catechol by CYP2C9, followed by the oxidization of the catechol to a reactive *ortho*-quinone metabolite (McDonald and Rettie, 2007). Tienilic acid is metabolized to reactive intermediates, the thiophene sulfoxide or the thiophene epoxide, by CYP2C9 (Koenigs et al., 1999). In recent studies, we developed useful in vitro cell-based assays using adenovirus to sensitively evaluate the involvement of CYP3A4 and superoxide dismutase 2 in drug-induced cytotoxicity (Yoshikawa et al., 2009; Hosomi et al., 2010). In the present study, a highly sensitive cytotoxicity assay system for CYP2C9-mediated metabolic activation was established in a similar way, and the drug-induced cytotoxicity was evaluated with the established assay system. Drugs investigated in this study were hepatotoxic drugs that are known to be CYP2C9 substrates (flutamide, fluvastatin, losartan, terbinafine, valproic acid, and zolpidem) and those that are known to be metabolically activated by CYP2C9 (benzbromarone and tienilic acid). As a result, we found for the first time that the cytotoxicity of losartan was enhanced by CYP2C9 and then performed additional studies to identify the structures of the reactive metabolites.

Materials and Methods

Chemicals and Reagents. Diclofenac, fluvastatin, and tienilic acid were obtained from Wako Pure Chemicals (Osaka, Japan). Losartan and terbinafine were obtained from LKT Laboratories (St. Paul, MN). Benzbromarone, flutamide, valproic acid, and zolpidem were obtained from Sigma-Aldrich (St. Louis, MO). Candesartan, eprosartan, irbesartan, telmisartan, and valsartan were obtained from Toronto Research Chemicals (Ontario, ON, Canada). Olmesartan was kindly provided by Daiichi-Sankyo (Tokyo, Japan). 4′-Hydroxydiclofenac and human CYP2C9 and CYP3A4 Supersomes (recombinant cDNA-expressed P450 enzymes prepared from a baculovirus insect cell system) were purchased from BD Gentest (Woburn, MA). The Adenovirus Expression Vector Kit (Dual Version) and adenovirus genome DNA-TPC were obtained from Takara Bio (Shiga, Japan). The QuickTiter Adenovirus Titer Immunoassay Kit was from Cell Biolabs (Tokyo, Japan). Stealth Select RNAi for Nrf2 (accession number NM_006164) and Stealth RNAi Negative Control Medium GC Duplex #2 were obtained from Invitrogen (Carlsbad, CA). Dulbecco's modified Eagle's medium was from Nissui Pharmaceutical (Tokyo, Japan). Restriction enzymes were from New England Biolabs (Ipswich, MA) and Takara Bio. All primers were commercially synthesized at Hokkaido System Sciences (Sapporo, Japan). Other chemicals were of analytical or the highest grade commercially available.

Cell Culture. Human embryonic kidney 293 cells and human hepatocarcinoma HepG2 cells were obtained from American Type Culture Collection (Manassas, VA). The 293 and HepG2 cells were maintained in Dulbecco's modified Eagle's medium containing 10% fetal bovine serum (Invitrogen), 3% glutamine, 16% sodium bicarbonate, and 0.1 mM nonessential amino acids (Invitrogen) in a 5% CO_2 atmosphere at 37°C. Cells were infected with the adenovirus in medium containing 5% fetal bovine serum.

Recombinant Adenovirus. A recombinant adenovirus expressing CYP2C9 (AdCYP2C9) was constructed using the cosmid-terminal protein complex method according to the manufacturer's instructions. CYP2C9 cDNA prepared by reverse transcription-polymerase chain reaction using total RNA from human liver obtained at autopsy was inserted into the SwaI site of the pAxcwtit vector. The use of human liver was approved by the ethics committees of Kanazawa University (Kanazawa, Japan) and Iwate Medical University (Morioka, Japan). The nucleotide sequences of CYP2C9 were confirmed by DNA sequence analysis (Long-Read Tower DNA sequencer; GE Healthcare, Little Chalfont, Buckinghamshire, UK). This vector and the parental adenovirus DNA terminal protein complex were cotransfected into 293 cells by Lipofectamine 2000 (Invitrogen). The recombinant adenovirus was isolated and propagated into the 293 cells. In a similar way, the recombinant adenovirus vector expressing a green fluorescence protein (GFP) was generated in the previous study (Hosomi et al., 2010). Viral titers were determined by a QuickTiter Adenovirus Titer Immunoassay Kit. The titers of AdCYP2C9 and AdGFP were 8.6×10^8 and 2.1×10^8 plaque-forming units/ml, respectively.

Immunoblot Analyses of Human CYP2C9 and Nrf2. SDS-polyacrylamide gel electrophoresis and immunoblot analyses of human CYP2C9, Nrf2, and GAPDH were performed. For human CYP2C9, total cell homogenates from adenovirus-infected HepG2 cells (5 μg) were separated on 7.5% polyacrylamide gels and electrotransferred onto a polyvinylidene difluoride membrane, Immobilon-P (Millipore Corporation, Billerica, MA). The membrane was probed with a polyclonal rabbit anti-human CYP2C9 antibody (Daiichi Pure Chemicals, Tokyo, Japan). Biotinylated anti-rabbit IgG and a VECTASTAIN ABC Kit (Vector Laboratories, Burlingame, CA) were used for diaminobenzidine staining. For human Nrf2, total cell homogenates from siRNA-transfected and adenovirus-infected HepG2 cells (25 μg) were separated on 7.5% polyacrylamide gels and electrotransferred onto a polyvinylidene difluoride membrane, Immobilon-P. The membrane was probed with polyclonal rabbit anti-human Nrf2 antibody (Santa Cruz Biotechnology, Inc., San Diego, CA), and the corresponding fluorescent dye-conjugated second antibody and an Odyssey infrared imaging system (LI-COR Biosciences, Lincoln, NE) were used for detection. For human GAPDH, SDS-polyacrylamide gel electrophoresis and immunoblot analysis were performed according to H. Hosomi, T. Fukami, A. Iwamura, M. Nakajima, and T. Yokoi (manuscript submitted for publication).

Diclofenac 4′-Hydroxylase Activity. HepG2 cells (3×10^5 cells/well) were seeded in 12-well plates. After a 24-h incubation, cells were infected with AdCYP2C9 or AdGFP for 1, 2, 3, or 5 days. Then, after a 1-h incubation with 100 μM diclofenac, the medium was subjected to high-performance liquid chromatography (HPLC) to measure the concentration of 4′-hydroxydiclofenac, a metabolite of diclofenac catalyzed by CYP2C9. The HPLC analysis was performed using an L-2130 pump (Hitachi, Tokyo, Japan), an L-2200 autosampler (Hitachi), and a D-2500 Chromato-Integrator (Hitachi) equipped with a Mightysil RP-18 C18 GP column (5-μm particle size, 4.6 mm i.d. × 150 mm; Kanto Chemical, Tokyo, Japan). The eluent was monitored at 280 nm. The mobile phase was 35% acetonitrile containing 20 mM sodium perchlorate (pH 2.5). The flow rate was 1.0 ml/min. The column temperature was 35°C. The retention times of 4′-hydroxydiclofenac and diclofenac were 8.1 and 22.8 min, respectively. The quantification of 4′-hydroxydiclofenac was performed by comparing the HPLC peak height with that of an authentic standard. The limit of quantification in the reaction mixture for 4′-hydroxydiclofenac was 250 nM with a coefficient of variation of <2%.

Cytotoxicity Assay. Nrf2 is known to regulate cytoprotective genes such as glutathione transferase, heme oxygenase-1, NAD(P)H:quinine oxidoreductase, superoxide dismutase, and UDP-glucuronosyltransferase (Copple et al., 2008). Our recent study demonstrated that drug-induced cytotoxicity could be detected with high sensitivity by the knockdown of Nrf2 in HepG2 cells (H. Hosomi, T. Fukami, A. Iwamura, M. Nakajima, and T. Yokoi, manuscript submitted for publication). Likewise, knockdown of Nrf2 was performed by siRNA transfection in this study. HepG2 cells were transfected with Stealth Select RNAi for Nrf2 (siNrf2) and Stealth RNAi Negative Control Medium GC Duplex #2 (siScramble) by Lipofectamine RNAiMAX Reagent (Invitrogen). According to the manufacturer's protocol, RNAi duplex-Lipofectamine RNAiMAX complexes were prepared and added to each well before the HepG2 cells were seeded (1.0×10^4 cells/well). The concentrations of siNrf2 and siScramble were 10 nM. After 24-h incubation, the cells were infected with AdCYP2C9 or AdGFP. Forty-eight hours after infection, the cells were treated with benzbromarone, tienilic acid, flutamide, fluvastatin, terbinafine, valproic acid, zolpidem, or sartans (candesartan, eprosartan, irbesartan, losartan, olmesartan, telmisartan, or valsartan) for 24 h. After incubation with the drugs, cell viability was quantified by 2-(2-methoxy-4-nitrophenyl)-3-(4-nitrophenyl)-5-(2, 4-disulfophenyl)-2*H*-tetrazolium monosodium salt (WST-8) and ATP assays according to the manufacturer's protocol. The WST-8 assay, which is a modified 3-(4,5-dimethylthiazol-2-yl)-2,5-diphenyltetrazolium assay, was performed using a Cell Counting Kit-8 (CCK-8 kit; Wako Pure Chemicals). After incubation with the drugs for 24 h, CCK-8 reagent was added and the absorbance of WST-8 formazan was measured at 450 nm. The ATP assay was performed using a CellTiter-Glo Luminescent Cell Viability Assay (Promega, Madison, WI). After incubation with the drugs for 24 h, CellTiter-Glo Reagent was added, and the generation of a luminescent signal